Systematics of putative euparkeriids (Diapsida: Archosauriformes) from the Triassic of China

The South African species *Euparkeria capensis* is of great importance for understanding archosaur evolution and the early radiation of archosauromorphs following the Permo–Triassic mass extinction, being placed by most phylogenetic analyses as the sister taxon to Archosauria (using a crown group definition) within the clade Archosauriformes. Although a number of species from Lower–Middle Triassic deposits worldwide have been referred to the putative family Euparkeriidae, the monophyly of this taxon is controversial and has yet to be demonstrated by quantitative phylogenetic analysis. Three Chinese taxa have been recently suggested to be euparkeriids: *Halazhaisuchus qiaoensis*, '*Turfanosuchus*' *shageduensis*, and *Wangisuchus tzeyii*, all three of which were collected from the Middle Triassic Ermaying Formation of northern China. Here, we reassess the taxonomy and systematics of these taxa. We regard '*Turfanosuchus*' *shageduensis* as a junior synonym of *Halazhaisuchus qiaoensis*, because no morphological features distinguish the two putative species and their holotypes emerge as sister taxa in a novel phylogenetic analysis. *Halazhaisuchus qiaoensis* is resolved as the sister taxon to *Euparkeria capensis*, forming a monophyletic Euparkeriidae that is in turn sister to Archosauria+Phytosauria. This is the first quantitative phylogenetic analysis to recover a non-monospecific, monophyletic Euparkeriidae, but euparkeriid monophyly is only weakly supported and will require additional examination. We regard *Wangisuchus tzeyii* as a *nomen dubium*, because the holotype is undiagnostic and there is no convincing evidence that the previously referred additional specimens represent the same taxon as the holotype. Our results have important implications for understanding the species richness and palaeobiogeographical distribution of early archosauriforms.

Title: Systematics of putative euparkeriids (Diapsida: Archosauriformes) from the Triassic of China

Authors and affiliations:

Roland B. Sookias[1,2], Corwin Sullivan[3], Jun Liu[3], Richard J. Butler[1,2]

1. School of Geography, Earth and Environmental Sciences, University of Birmingham, Edgbaston, Birmingham B15 2TT, UK; email: sookias.r.b@gmail.com; phone: +441214146152

2. GeoBio-Center, Ludwig-Maximilians-Universität München, Richard-Wagner-Str. 10, 80333 Munich, Germany

3. Key Laboratory of Vertebrate Evolution and Human Origins of Chinese Academy of Sciences, Institute of Vertebrate Paleontology and Paleoanthropology, Chinese Academy of Sciences, 100044 Beijing, China

Corresponding author: Roland B. Sookias; address: School of Geography, Earth and Environmental Sciences, University of Birmingham, Edgbaston, Birmingham B15 2TT, UK; email: sookias.r.b@gmail.com; phone: +441214146152

Abstract: The South African species *Euparkeria capensis* is of great importance for understanding archosaur evolution and the early radiation of archosauromorphs following the Permo–Triassic mass extinction, being placed by most phylogenetic analyses as the sister taxon to Archosauria (using a crown group definition) within the clade Archosauriformes. Although a number of species from Lower–Middle Triassic deposits worldwide have been referred to the putative family Euparkeriidae, the monophyly of this taxon is controversial and has yet to be demonstrated by quantitative phylogenetic analysis. Three Chinese taxa have been recently suggested to be euparkeriids: *Halazhaisuchus qiaoensis*, '*Turfanosuchus*' *shageduensis*, and *Wangisuchus tzeyii*, all three of which were collected from the Middle Triassic Ermaying Formation of northern China. Here, we reassess the taxonomy and systematics of these taxa. We regard '*Turfanosuchus*' *shageduensis* as a junior synonym of *Halazhaisuchus qiaoensis*, because no morphological features distinguish the two putative species and their holotypes emerge as sister taxa in a novel phylogenetic analysis. *Halazhaisuchus qiaoensis* is resolved as the sister taxon to *Euparkeria capensis*, forming a monophyletic Euparkeriidae that is in turn sister to Archosauria+Phytosauria. This is the first quantitative phylogenetic analysis to recover a non-monospecific, monophyletic Euparkeriidae, but euparkeriid monophyly is only weakly supported and will require additional examination. We regard *Wangisuchus tzeyii* as a *nomen dubium*, because the holotype is undiagnostic and there is no convincing evidence that the previously referred additional specimens represent the same taxon as the holotype. Our results have important implications for understanding the species richness and palaeobiogeographical distribution of early archosauriforms.

Keywords: Euparkeriidae, Archosauriformes, Triassic, China, *Euparkeria*

45 **Main text:**

46

47 **Introduction**

48

49 *Euparkeria capensis* from the early Anisian (Middle Triassic) of South Africa (Ewer 1965;
50 Sookias & Butler 2013) is a key species of early archosauriform that is widely regarded as
51 approaching the ancestral archosaur body plan (e.g. Romer 1972; Norman & Weishampel 1991;
52 Parrish 1997). *E. capensis* falls immediately outside of or very close to Archosauria in most
53 phylogenetic studies (e.g. Gower & Wilkinson 1996; Bennett 1996; Benton 1999; Nesbitt 2011;
54 Brusatte et al. 2010; Ezcurra, Lecuona, & Martinelli, 2010), and has been used as an outgroup in
55 numerous studies of archosaur phylogeny and morphological evolution (e.g. Perry 1992; Carrier
56 ~~and~~ Farmer 2000; Hutchinson 2001a,b; Marugán-Lobón & Buscalioni 2003; Nesbitt 2003;
57 Rauhut 2003; Seymour et al. 2004; de Ricqlès et al. 2008; Sullivan 2010; Maidment & Barrett
58 2011; Butler, Barrett, & Gower, 2012; Foth ~~and~~ Rauhut 2013). Several other taxa from Lower–
59 Middle Triassic deposits around the world have historically been assigned to the family
60 Euparkeriidae (reviewed by Sookias ~~and~~ Butler 2013; see also Sookias et al. 2014), although no
61 cladistic analysis has yet recovered this taxon as a monophyletic, non-monospecific entity. Most
62 previous quantitative phylogenetic analyses of basal archosauriforms have not tested the
63 monophyly of Euparkeriidae, because they have not included putative euparkeriid species from
64 Poland, Russia and China (~~Sookias and Butler 2013~~; but see Sookias et al. 2014). The inclusion
65 of these putative euparkeriid species in phylogenetic analyses has been hampered by the often
66 fragmentary nature of their remains, and an ongoing lack of clarity with regard to their taxonomy
67 and anatomy (Gower ~~and~~ Sennikov 2000; Sookias ~~and~~ Butler 2013).

Three Chinese taxa from the Anisian Ermaying (see Table S2 names in Chinese characters, Pinyin and previously used romanizations) Formation of north central China have been recently considered as putative euparkeriids worthy of further investigation (Sookias and Butler 2013): *Wangisuchus tzeyii* Young 1964, *Halazhaisuchus qiaoensis* Wu 1982, and '*Turfanosuchus*' *shageduensis* Wu 1982. However, the phylogenetic relationships of these Chinese putative euparkeriids to each other, and to other archosauriforms, have never previously been tested. Given the pivotal phylogenetic position of *Euparkeria capensis*, testing the affinities of these taxa has the potential to clarify the relationships of major clades of early archosauriforms and patterns of character evolution during the rise of Archosauria. Here we revise the taxonomy and review the anatomy of the Chinese putative euparkeriids. We also conduct a novel phylogenetic analysis of early archosauriforms that includes two of these taxa, shedding new light on their systematic positions.

Taxonomic history of the Chinese euparkeriids

The three species discussed here all derive from the Ermaying Formation of China and were referred to Euparkeriidae in their original descriptions. *Wangisuchus tzeyii* from the upper Ermaying Formation was described by Young (1964) and referred to Euparkeriidae on the basis of supposed similarities in the maxilla and pelvic girdle to *Euparkeria capensis*. *Wangisuchus tzeyii* has often been subsequently considered to represent a "rauisuchian" or other pseudosuchian (i.e. a member of the 'crocodile-line' of Archosauria), based primarily on the presence of a suchian calcaneum within material questionably referred to this taxon (e.g. Welles and Long, 1974; Krebs 1976; Parrish 1992; Gower 2000; Gower & Sennikov 2000; Borsuk-Białynicka &

Sennikov 2009; Nesbitt 2011; Nesbitt et al. 2013). However, the species has never been adequately reassessed (Sookias & Butler 2013) and various authors have continued to consider *Wangisuchus tzeyii* a possible euparkeriid and utilize this referral in biogeographic and biostratigraphic analyses (e.g. Sennikov 1989a,b; Shubin ~~and~~ Sues 1991; Lucas 1998, 2001). The species was cited as one of the earliest records of any archosaur (as a "rauisuchian") by Benton & Donoghue (2007), and used as evidence for constraining the timing of the crocodile-bird split.

Halazhaisuchus qiaoensis and '*Turfanosuchus*' *shageduensis* were described by Wu (1982) and referred to Euparkeriidae based on similarities to *Euparkeria capensis*, including plesiomorphies such as retention of intercentra and a "large coracoid" (Wu 1982, p. 20). Zhen et al. (1985) considered *Halazhaisuchus qiaoensis* to be a "thecodont" relatively closely related to the proterosuchid *Chasmatosaurus yuani*, although no anatomical justification for this was given. Sennikov (1989a,b) referred *Halazhaisuchus qiaoensis*, '*Turfanosuchus*' *shageduensis* and *Wangisuchus tzeyii* (as well as *Xilousuchus sapingensis*; see below) to the euparkeriid subfamily Dorosuchinae, along with *Dorosuchus neoetus* from the Middle Triassic of Russia. The basis for the referral was that these taxa were supposedly more robust than *Euparkeria capensis*. Parrish (1993) was apparently confusing *Halazhaisuchus qiaoensis* with '*Turfanosuchus' shageduensis* when he stated that the latter was a primitive archosauriform distinct from *Turfanosuchus dabensis* based on the presence of vertebral intercentra "and other features" (Parrish 1993, p. 297), given that intercentra are present in *Halazhaisuchus qiaoensis* but not in '*Turfanosuchus*' *shageduensis*. Lucas (2001) considered both *Halazhaisuchus qiaoensis* and '*Turfanosuchus*' *shageduensis* as euparkeriids, together with *Wangisuchus tzeyii* and *Euparkeria capensis* (see also Lucas 1998). Wu and Russell (2001) compared the anatomy of *Halazhaisuchus qiaoensis* and '*Turfanosuchus*' *shageduensis* to that of *Turfanosuchus dabanensis*. They noted resemblances in humeral and femoral morphology between the first two species and *Turfanosuchus dabanensis*,

but also identified differences including the presence of intercentra in *Halazhaisuchus qiaoensis* and discrepancies in osteoderm morphology between *Halazhaisuchus qiaoensis* and *Turfanosuchus dabanensis*. Borsuk-Białynicka and Evans (2003) tentatively supported the referral of *Halazhaisuchus qiaoensis* to Euparkeriidae, whilst Borsuk-Białynicka and Evans (2009) regarded the euparkeriid affinities of the taxon as doubtful.

Several other taxa from the Chinese Triassic and Lower Jurassic have historically been assigned to Euparkeriidae but are no longer regarded as potential members of the group and are ~~not~~ discussed in detail here. *Xilousuchus sapingensis* Wu 1981 was assigned to Euparkeriidae by Sennikov (1989a,b), but recent analyses have reidentified it as a ctenosauriscid poposauroid (Butler et al. 2011; Nesbitt 2011; Nesbitt, Liu, & Li 2011). *Platyognathus hsui* Young 1944 was referred to Euparkeriidae by Huene (1956), but this taxon is a crocodyliform (Wu & Sues 1996). *Turfanosuchus dabanensis* Young 1973 was initially assigned to Euparkeriidae, but was regarded by Parrish (1993) as a suchian. The species was redescribed by Wu & Russell (2001) as a non-pseudosuchian not closely related to *E. capensis*, but was placed in Pseudosuchia by the most recent and extensive phylogenetic analysis of Archosauriformes (Nesbitt 2011), and has since been identified as a member of the pseudosuchian clade Gracilisuchidae (Butler et al. 2014). '*Fukangolepis*' *barbaros* Young 1978 was mentioned as having been referred to Euparkeriidae by Parrish (1986) but presumably this was a *lapsus calami* given that the holotype of the species is an indeterminate dicynodont skull fragment (Lucas & Hunt 1993) assigned by Young (1978) to Aetosauria; the fact that Parrish (1986) cites Young (1973) for this assertion indicates Parrish may have confused '*Fukangolepis*' *barbaros* with *Turfanosuchus dabanensis*. Finally, *Yonghesuchus sangbiensis* Wu, Liu and Li 2001 was listed without discussion as a euparkeriid by Wu & Sun (2008), but this taxon is also a gracilisuchid pseudosuchian (Butler et al. 2014).

Geological setting

All of the Chinese putative euparkeriid specimens discussed here are from the Ermaying Formation, which was deposited during the Triassic in a meandering fluvial environment with an east to west palaeocurrent (Liu et al. 2012). The specimens assigned to *Halazhaisuchus qiaoensis* (IVPP V6027) and '*Turfanosuchus*' *shageduensis* (IVPP V6028) are from the sandstones of the lower Ermaying Formation. The lower Ermaying formation is made up of yellowish pink, yellowish green and greyish white quartz arkose (Yin 2003). The lower Ermaying Formation has been considered early Anisian in age as a result of long-range biostratigraphic correlation with Subzone B of the *Cynognathus* Assemblage Zone of South Africa, based primarily on the presence of the dicynodont *Kannemeyeria* (Rubidge 2005; Fröbisch 2009). Dating of Subzone B of the *Cynognathus* Assemblage Zone is itself based on long-range vertebrate biostratigraphy (Hancox 2000). Lucas (2001) argued for an Olenekian date for the lower Ermaying based on the presence of the dicynodont *Shansiodon* in the upper Ermaying (see below). Sues and Fraser (2010) concurred with this age assessment, based on a proposed correlation of the upper Heshanggou Formation of northern China with the lower Ermaying Formation and the presence of the typically Olenekian spore-bearing tree *Pleuromeia sternbergii* in the former. However, Butler et al. (2011) noted that *Pleuromeia sternbergii* extends into the early Anisian in Germany, and that at least part of the Heshanggou Formation may be Anisian in age. Using sensitive, high-resolution ion microprobe (SHRIMP) U-Pb dating, the age of the upper Ermaying Formation (Member II) was recently found to be 245.9 ± 3.2 Ma (Liu, Li, & Li, 2013). Although the range of error encompasses the entire Anisian (currently dated as 247.2–242 Ma: Cohen, Finney, & Gibbard, 2013), this result supports an Anisian date for the upper Ermaying, and by inference an early Anisian or late Olenekian date for the lower Ermaying and Heshanggou formations.

All material referred to *Wangisuchus tzeyii* is from the white sandstones and mudstones of the upper Ermaying Formation. Hancox et al. (2013) and Rubidge (2005) assigned the upper Ermaying Formation to the late Anisian based on the presence of the dicynodont *Shansiodon*. The same genus occurs in Subzone C of the *Cynognathus* Assemblage Zone of South Africa (Hancox, Angielczyk, & Rubidge, 2013), and the shansiodont *Vinceria* occurs in the Río Mendoza and Upper Puesto Viejo formations of Argentina (Renaut ~~and~~ Hancox 2001; Hancox 1998). The proposed late Anisian date for Subzone C of the *Cynognathus* Assemblage Zone is itself based on long-range vertebrate biostratigraphy (Hancox 2000). The upper Ermaying Formation was referred to the Perovkan land-vertebrate faunochron by Lucas (2010), again based upon vertebrate biostratigraphy. As noted above, new SHRIMP analyses have confirmed an Anisian date for the upper Ermaying Formation.

Terminology and methods

We use the limb orientation terminology of Gower (2003), which combines that of Romer (1942) and that of Rewcastle (1980). This orientation corresponds to a fully anteriorly extended hindlimb (the anterior surfaces of hindlimb bones in descriptions of fully erect taxa such as dinosaurs thus correspond to the dorsal surfaces in our terminology), and a forelimb with the humerus fully extended posteriorly and the epipodials fully extended anteriorly (the anterior surfaces of forelimb bones in fully erect taxa thus correspond to the ventral surface of the humerus and to the dorsal surfaces of the radius and ulna here). The scapula is described with the shaft held vertically. We use the terminology of Wilson (1999) for vertebral laminae and that of Wilson et al. (2011) for vertebral fossae.

Phylogenetic analyses were carried out using the matrix of Butler et al. (2014), modified from Nesbitt (2011), with *Halazhaisuchus qiaoensis* and '*Turfanosuchus*' *shageduensis* (not previously included by Nesbitt [2011] or Butler et al. [2014]) included in separate analyses as both distinct taxa and as a combined taxon. Additionally, we changed the scoring of osteoderm shape in *Euparkeria capensis* from that used by Nesbitt (2011: character 407) from "square-shaped, about equal dimensions" to "longer than wide" (see Discussion). The analyses were conducted in TNT v. 1.1 (Goloboff, Farris, & Nixon, 2003; 2008). We employed the same methodology as Nesbitt (2011), eliminating the same taxa from the dataset prior to analysis, with the same characters treated as ordered, and using equally weighted parsimony. An initial search using the "New Technology search" option was carried out using sectorial search, ratchet and tree-fusing options with default parameters. Minimum tree length was obtained for 1000 separate replicates and the trees were stored in RAM. A heuristic tree search was then conducted using the stored trees, followed by TBR branch swapping. Standard bootstrap values and Bremer support values (decay indices) were calculated for each node using the inbuilt functionality of TNT and the BREMER script respectively.

Institutional abbreviations

IVPP, Institute of Vertebrate Paleontology and Paleoanthropology, Chinese Academy of Sciences, Beijing, China; SAM, Iziko South African Museum, Cape Town, South Africa; SMNS, Staatliches Museum für Naturkunde, Stuttgart, Germany; UMZC, University Museum of Zoology, Cambridge, UK.

Systematic palaeontology

ARCHOSAUROMORPHA von Huene, 1946 sensu Gauthier, Kluge, & Rowe1988

ARCHOSAURIFORMES Gauthier, Kluge, & Rowe, 1988 sensu Nesbitt, 2011

‘*Wangisuchus*’ Young, 1964

[Nomen dubium]

Type and only species. ‘*Wangisuchus tzeyii*’ Young, 1964.

‘*Wangisuchus tzeyii*’ Young, 1964

[Nomen dubium]

Holotype. IVPP V2701, an incomplete left maxilla lacking teeth.

Syntypes. IVPP V2702-V2704, maxillae (paratypes).

Horizon and locality. All specimens assigned to *Wangisuchus tzeyii* are from the upper Ermaying Formation of Shanxi Province (Middle Triassic: Anisian). IVPP V2701 (holotype) and IVPP V2702-V2704 (paratypes) are from locality 56173, Xishiwa near Louzeyu Village, Wuxiang

County (Fig. 1). This locality has been entered in the *Paleobiology Database* as number 101059. See Geological *Setting for further information.*

Remarks. The holotype maxilla, IVPP V2701 (Fig. 2A–B), is fragmentary and undiagnostic, as are the paratype specimens. Whilst the presence of alveoli and interdental plates indicates thecodont tooth implantation (a synapomorphy of *Erythrosuchus*+Archosauria: Nesbitt 2011), neither a suite of autapomorphies nor a unique combination of character states can be identified in the maxilla. The original diagnosis presented by Young (1964) was inadequate for a number of reasons: it referred to the "long and low" shape of the maxilla, but the holotype maxilla does not differ in this regard from those of most early archosauriforms; the posterior process of the maxilla was described as "pointed", but is in fact incomplete; the anterior margin of the maxilla was described as "rounded" but is also incomplete; and teeth and other elements not preserved in the holotype were used in the diagnosis, but there is no convincing case for referring these elements to the same taxon as the holotype. We therefore consider '*Wangisuchus tzeyii*' to be a nomen dubium. The most exclusive phylogenetic placement that can be reasonably supported for the holotype is Archosauriformes indet., based on the inferred presence of thecodont dental implantation in the maxilla. As noted above, this feature supports a position crownward of *Proterosuchus* (Nesbitt 2011).

Young (1964) referred many isolated and poorly preserved postcranial elements from the type locality and other localities in the same region to '*Wangisuchus tzeyii*', but first-hand inspection of much of this material revealed it to be undiagnostic. Furthermore, there are no compelling similarities to justify regarding even the two relatively complete paratype maxillae (IVPP V2703, V2704) as necessarily conspecific with the holotype, and in fact both of these paratype maxillae appear to differ from the holotype in having a convex rather than straight

anterodorsal margin as discussed by several authors (Kuhn 1976; Parrish 1993; Gower and Sennikov 2000; Nesbitt 2011), an unnumbered calcaneum within this previously referred material demonstrably belongs to a suchian archosaur, but there is no evidence to support the referral of this calcaneum to '*Wangisuchus tzeyii*'.

EUPARKERIIDAE von Huene, 1920 sensu Sookias and Butler 2013

Halazhaisuchus Wu, 1982

Type and only species. *Halazhaisuchus qiaoensis* Wu, 1982.

Halazhaisuchus qiaoensis Wu, 1982

Synonymy. Turfanosuchus shageduensis Wu, 1982 (junior subjective synonym).

Holotype. IVPP V6027, posterior three cervical and anterior three dorsal vertebrae in articulation with osteoderms and incomplete ribs (V6027-1), seven dorsal vertebrae in articulation with osteoderms (V6027-2), left (V6027-3) and right (V6027-4) scapulae, left (V6027-3) and partial right (V6027-4) coracoids, right humerus (V6027-5), ulna (V6027-6), and radius (V6027-7), an

273 isolated left cervical rib (V6027-8), and an isolated median osteoderm (V6027-9). All material
274 probably pertains to a single individual.

275

276 *Referred specimen.* IVPP V6028 (holotype of *Turfanosuchus shageduensis* Wu, 1982), mostly
277 complete right mandible (V6028-1), six cervical vertebrae missing upper neural arches and neural
278 spines (V6028-2), right scapula (V6028-3), coracoid (V6028-3), humerus (V6028-4), radius
279 (V6028-7/8/9; note that the correct subnumbers for the radius, ulna and fibula are uncertain), ulna
280 (V6028-7/8/9), femur (V6028-5), tibia (V6028-6) and fibula (V6028-7/8/9). All material
281 probably pertains to a single individual.

282

283 *Horizon and locality.* IVPP V6027 is from Fugu County, Shaanxi Province, China (Fig. 1), and
284 IVPP V6028 is from Jungar Banner, Nei Mongol *Autonomous Region, China (Fig. 1). Both are*
285 *from the lower* Ermaying Formation (Lower or Middle Triassic: late Olenekian or early Anisian).
286 *Both localities have been entered into the Paleobiology Database*, *as locality numbers* 100138
287 and 92436. *See Geological Setting for further information.*

288

289 *Original diagnosis.* Relatively small pseudosuchian. Pectoral girdle well developed. Scapula
290 exceptionally elongated and strongly expanded at both ends; ratio of scapula to humerus over
291 1.15:1; oval muscle-attachment area above glenoid with notably projecting ridge. Coracoid very
292 large, forming two thirds of glenoid. Humerus robust, terminating in triangularly expanded apex
293 proximally due to well-developed deltopectoral crest along proximal quarter of shaft. Radius and
294 ulna slender, ulna with well-developed olecranon process. Vertebrae slightly amphicoelous, with
295 elongated centra and low neural spines expanded distally; presacral vertebrae with intercentra.
296 Cervical and anterior dorsal ribs three-headed. Row of dorsal scutes on either side of midline,

297 scutes overlap one another and are leaf-like in outline; posterior ends of scutes grooved ventrally;
298 in cervical and anterior dorsal regions scutes from both sides are sutured together firmly
299 (paraphrased from Wu 1982).
300
301 *Revised diagnosis.* Relatively small (femur length 127 mm) archosauriform diagnosable on the
302 basis of two autapomorphies: (1) strongly pronounced tuber on the scapula, for attachment of the
303 scapular head of the *m. triceps*, that is circular in outline when the scapula is in lateral view, with
304 the apex of the tuber slightly depressed; (2) pronounced muscle attachment scar on the scapula in
305 the form of a depressed strip on the lateral surface of the blade running from anterodorsal to
306 posteroventral, beginning at an abrupt kink in the anterior margin at around midlength of the
307 blade. The species is further diagnosable on the basis of the following unique combination of
308 characters: two rows of paramedian scutes that are longer than wide, taper to an anterior process
309 anteriorly and are broad and rounded posteriorly, with a longitudinal keel closer to the medial
310 margin than the lateral one; large flattened flange projecting from the proximal part of the
311 anterior margin of each cervical rib; presence of a tuber on the scapula for attachment of the
312 scapular head of the *m. triceps*; presence of dorsal intercentra.
313
314 *Remarks.* IVPP V6028 was designated by Wu (1982) as the holotype of a putative new species of
315 the genus *Turfanosuchus*, '*T.*'*shageduensis*. The type species of *Turfanosuchus*, *Turfanosuchus*
316 *dabanensis*, is from the Kelamayi Formation (Middle Triassic) of Xinjiang, China. Subsequently
317 Gower & Sennikov (2000) expressed doubts that '*Turfanosuchus' shageduensis* and
318 *Turfanosuchus dabanensis* were congeneric, and noted instead the strong similarities of
319 '*Turfanosuchus' shageduensis* to *Halazhaisuchus qiaoensis* from the same formation. We
320 synonymize *Halazhaisuchus qiaoensis* and '*Turfanosuchus*' *shageduensis* on the basis that there

321 are no morphological features that distinguish the two nominal species with certainty (all possible
322 differences are minor and can be ascribed to preservation and/or intraspecific variation) and that
323 the two nominal species group as sister taxa just outside Archosauria in a phylogenetic analysis.
324 *Turfanosuchus dabanensis* is by contrast placed phylogenetically distant from *Halazhaisuchus*
325 *qiaoensis* and '*Turfanosuchus*' *shageduensis* as part of Archosauria (see below). *Halazhaisuchus*
326 *qiaoensis* and '*Turfanosuchus*' *shageduensis* were originally named in the same paper (Wu 1982),
327 and we consider *Halazhaisuchus qiaoensis* to be the valid senior subjective synonym based on
328 page priority. Wu (1982) distinguished the two nominal species primarily based on the presence
329 of intercentra and dorsal osteoderms in *Halazhaisuchus qiaoensis*, in contrast with the supposed
330 absence of these features in '*Turfanosuchus*' *shageduensis*. However, both osteoderms and
331 intercentra can easily be lost during preservation, and the highly incomplete and poorly preserved
332 nature of IVPP V6028 ('*Turfanosuchus*' *shageduensis*) suggests that taphonomic removal is a
333 particularly likely possibility in this case. IVPP V6028 has even suffered post-mortem loss of the
334 dorsal portions of the preserved vertebrae, above which any osteoderms would have lain.
335 Moreover, intercentra are absent in the cervical vertebrae of IVPP V6027 (*Halazhaisuchus*
336 *qiaoensis*), and the only vertebrae that are preserved in IVPP V6028 are from the cervical region.
337 The strata bearing both taxa are of the same age and are not widely separated
338 palaeogeographically, making synonymization even more parsimonious as an alternative to
339 retaining '*Turfanosuchus*' *shageduensis* as a separate species.

340 The original differential diagnosis of *Halazhaisuchus qiaoensis* was insufficient because it
341 did not adequately distinguish the taxon from other stem- and early archosaurs. Many features
342 listed (e.g. "pectoral girdle well-developed") were not sufficiently clear or distinct to be effective
343 in diagnosing the taxon. Other features are shared with other taxa: leaf-shaped osteoderms and
344 presacral intercentra are shared with *Euparkeria capensis* (Ewer 1965), and the vertebral features

345 listed in the original diagnosis are essentially also shared with *Euparkeria capensis* (Ewer 1965;
346 UMZC T.692).

347 However, the exact shape of the *m. triceps* attachment tuber is identified here as
348 autapomorphic, because although corresponding tubera are present in other basal archosauriform
349 taxa (e.g. *Batrachotomus kupferzellensis*, Gower ~~and~~ Schoch 2009), they differ in form.
350 Similarly, the muscle attachment scar on the blade of the scapula described here as
351 autapomorphic in form is much more pronounced than in any other early archosauriform that we
352 have examined. We have also identified a combination of features present in *Halazhaisuchus* that
353 distinguishes it from other taxa. For example, although *Euparkeria capensis* possesses similarly-
354 shaped osteoderms, it lacks an *m. triceps* tuber (Ewer 1965). Osteoderm morphology
355 distinguishes *Halazhaisuchus qiaoensis* from many other taxa (e.g. *Batrachotomus*
356 *kupferzellensis*, in which the osteoderms are blunter anteriorly), and the presence of anterior
357 flanges on the cervical ribs differentiates *Halazhaisuchus qiaoensis* from some other non-
358 archosaurian archosauriforms such as *Chanaresuchus bonapartei* (Romer 1972) and
359 *Erythrosuchus africanus* (Gower 2003).

360

361

362 **Description**

363

364 *Mandible.* IVPP V6028-1 (Fig. 3; measurements for this and all other elements given in Table S1)
365 is a poorly preserved right mandibular ramus lacking the posteriormost part. Extensive cracking
366 and damage to the external surfaces of most elements prevents accurate identification of sutures.
367 The mandible is ventrally convex in lateral view. The ramus is long anteroposteriorly and shallow

dorsoventrally, but the heavily damaged and compressed posterior end of the ramus was probably deeper in life. A mandibular fenestra cannot be identified with certainty due to poor preservation. At least five teeth (Fig. 3, t) and three additional empty alveoli can be identified, and the dentary appears to be long enough to accommodate around 12 teeth in total, but the exact posterior extent of the dentary is unclear. The teeth are close to circular in cross-section, but further details of their morphology cannot be discerned. The prearticular (Fig. 3, pra) can be identified posteriorly on the medial side, expanding in dorsoventral depth towards its posterior end. The prearticular is mediolaterally thin and dorsoventrally deep with an almost flat (very slightly medially convex in posterior view) and smooth medial surface. An abrupt, approximately longitudinal step (Fig. 3, step) demarcates a slightly inset ventral portion of the medial surface of the prearticular that would have been covered by the angular in the intact mandible.

Contributing to the anterior portion of the ramus are fragments of bone, which based on their positions probably represent parts of the splenial (Fig. 3, sp) and coronoid (Fig. 3, c); the part of the ramus formed by these elements is medially convex in posterior view. The possible coronoid medial to the tooth row is transversely wider in dorsal view than is the part of the dentary lateral to the tooth row. The ventrolateral edge of the dentary (Fig. 3, d) is convex in anterior view. Ventrally, the dentary and splenial (Fig. 3, sp) are separated by a narrow gap, but this may be due to post-mortem damage. The dorsolateral edge of the area of the mandibular ramus that is likely formed by the surangular (Fig. 3, sa) is convex in anterior view, and was clearly dorsally convex in lateral view when intact. The area of the mandibular ramus that is likely formed by the angular (Fig. 3, a) forms the ventralmost point of the jaw. The lateral surface of the angular is dorsoventrally convex, and the angular tapers posteriorly in lateral view.

391 *Cervical vertebrae.* IVPP V6027-1 (Fig. 4A–E) includes what we identify as the articulated
392 posterior three cervical vertebrae (in articulation with what we identify as the anterior three
393 dorsals; the exact point of the cervical-dorsal transition is hard to pinpoint with certainty) and
394 IVPP V6028-2 (Fig. 4K–O) consists of six very poorly preserved, articulated cervical vertebrae,
395 all of which lack the dorsal part of the neural arch including the neural spine. The neurocentral
396 sutures are fused. The centra of the cervical vertebrae are spool-shaped and longer than tall, with
397 a low ventral keel. In the anterior cervicals the diapophysis (Fig. 4A–K, di) is placed near the
398 anterodorsal corner of the centrum, and the parapophysis (Fig. 4A–K, pa) is placed near the
399 anteroventral corner; posteriorly along the column the diapophysis moves posterodorsally, the
400 parapophysis moves dorsally to approximately halfway up the centrum, and the two become
401 connected by a variably developed paradiapophyseal lamina (Fig. 4A, ppdl). A thick, rounded
402 prezygadiapophyseal lamina (Fig. 4A, prdl) connects the prezygapophysis and the diapophysis. A
403 shallow spinodiapophyseal fossa (Fig. 4A, sdf) is present immediately dorsal to the diapophysis.
404 The anterior and posterior articular facets of the centra are gently concave and subcircular. Some
405 of the postzygapophyses bear epipophyses (Fig. 4A, ep), but these do not extend posteriorly
406 beyond the postzygapophyseal articular surfaces. The neural spines (Fig. 4A–B, ns) widen
407 transversely towards their distal ends to form broad, flat spine tables, each of which attains its
408 maximum transverse width at a point slightly anterior to the midlength. No intercentra can be
409 identified between the cervical vertebrae, although their absence could be preservational. The
410 vertebrae of IVPP V6028-2 are slightly longer and lower in their proportions than those of IVPP
411 V6027-1, but this appears to be due to post-mortem compression of the former given that their
412 ventral surfaces are flattened; thus no differences in cervical vertebral morphology separate the
413 two individuals.

414

Cervical ribs. IVPP V6027-1 (Fig. 4A–E) includes three partial cervical ribs in articulation with vertebrae and IVPP V6027-8 (Fig. 5A–B) consists of a single left cervical rib. The cervical ribs are two-headed and their shafts extend posteriorly, ventrally and laterally and are gently curved posteriorly, especially towards their distal ends. The tuberculum is longer than the capitulum (Fig. 5, tub, cap) and is directed medially whereas the capitulum is directed anteromedially. A dorsoventrally thin flange (Fig. 5, fl), which widens transversely as it continues proximally, extends along the anterolateral margin of each rib. A similar structure is present in several other archosauriforms, including *Batrachotomus kupferzellensis* (Gower & Schoch 2009, fig. 2M; SMNS 91046), *Gracilisuchus stipanicicorum* (Romer 1972, fig. 7), and *Smilosuchus gregorii* (Nesbitt 2011, fig. 28J).

Dorsal vertebrae. IVPP V6027-1 (Fig. 4A–E) includes what are probably the anteriormost three dorsal vertebrae in articulation, and IVPP V6027-2 (Fig. 4F–J) consists of seven mid to posterior dorsal vertebrae. The dia- and parapophyses (Fig. 4A,F, di, pa) are close together in the anteriormost vertebra of IVPP V6027-2, indicating that this vertebra is already a mid- or posterior dorsal. In the posteriormost vertebra of IVPP V6027-1, by contrast, the dia- and parapophyses are relatively well-separated, and at least the posterior two dorsal vertebrae (what we regard here as the anteriormost dorsal may in fact be the posteriormost cervical – identification of the exact point of transition is difficult) preserved in this specimen can be unequivocally identified as anterior dorsals because they are in articulation with the posteriormost cervicals. Accordingly, IVPP V6027-1 and V6027-2 cannot be combined to form a continuous dorsal series.

The anterior dorsal vertebrae are generally similar to the cervical vertebrae described above, but differ in that the diapophyses are longer and dorsoventrally compressed, and are situated higher and further back on the centrum, on the suture with the neural arch. These

differences with respect to the cervical vertebrae become more pronounced posteriorly along the dorsal column. In successively more posterior presacral vertebrae the diapophysis and parapophysis become gradually joined, first being connected by a paradiapophyseal lamina (Fig. 4 A, F, ppdl; already present in the more posterior cervical vertebrae) and then fusing entirely to form a single apophysis. The latter condition is present by the fourth vertebra in IVPP V6027-2, although in this vertebra the parapophysis and diapophysis remain distinguishable as components of the apophysis. The diapophysis and parapophysis are indistinguishable from the fifth vertebra of IVPP V6027-2 onwards. A low anterior centroparapophyseal lamina (Fig. 4A, F, acpl) connects the parapophysis (and in more posterior vertebrae, the single fused apophysis) to the anterior margin of the centrum. A thick, rounded prezygadiapophyseal lamina (Fig. 4A,F, prdl) connects the prezygapophysis and the diapophysis. A spinodiapophyseal fossa (Fig. 4F, sdf) is present dorsal to the diapophysis in the third and fifth preserved vertebrae, ~~but the~~ presence of this structure in other vertebrae is difficult to assess due to damage. The plane of articulation between the zygapophyses is roughly horizontal, rather than inclined as in the cervical vertebrae. Intercentra (Fig. 4F, H, ic) are preserved in apparent articulation posterior to the fourth, fifth and sixth vertebrae of IVPP V6027-2; they are mediolaterally elongated ovals in ventral view, and their lateral tips curve dorsally which would have made them crescentic in anterior or posterior view. The dorsal ends of the neural spines (Fig. 4F,G, ns) are expanded into anteroposteriorly elongated oval spine tables that are covered in rugosities.

Scapula. IVPP V6027-3 (Fig. 6A–B) is a left scapula in articulation with the coracoid, and IVPP V6027-4 is a right scapula (Fig. 6C–D). IVPP V6028-3 is a right scapula in articulation with a partial coracoid (Fig. 6E–F). The scapula is long and bladelike, and the shaft is waisted at its dorsoventral midpoint in lateral view. In posterior view the shaft of the scapula arcs in a medially

concave curve. The scapulae of IVPP V6027 each possess a pronounced posterolaterally directed tuber placed immediately dorsal to the glenoid along the posterior margin of the bone (Fig. 6A–D, tu; the tuber on the left scapula is damaged). This tuber is for attachment of the scapular head of the *m. triceps*, and has a depressed lateral surface that is circular in outline in lateral view. The acromion process (Fig. 6C–F, acr) is larger and more prominent than in *Euparkeria capensis* (SAM-PK-5867). The lateral surface of the scapula bears a muscle attachment area (Fig. 6A,C, mar) in the form of a parallel ridge and groove. The groove is situated just anteroventral to the ridge, and both extend posteroventrally from a point on the anterior margin of the scapula that lies about two thirds of the way down from the dorsal end and coincides with the level at which the shaft is anteroposteriorly narrowest. On the medial surface a similarly oriented muscle attachment ridge (Fig. 6B,D, mar) begins on the anterior margin around two thirds of the way up from the ventral end, and terminates at the anteroposteriorly narrowest point of the shaft just anterior to the posterior margin. The posterior part of the shaft is substantially thicker transversely than the anterior part. The proximal end of the shaft is strongly thickened transversely in the glenoid region, which articulates with a similarly thickened part of the coracoid.

The scapula of IVPP V6028-3 is poorly preserved. The margin of the bone is broken in the region in which the tuber for the *m. triceps* would have been placed, but there is a swelling in this position that probably represents what remains of the tuber after post-mortem damage. The muscle attachment ridges identified in IVPP V6027 are not visible in IVPP V6028-3, but this is almost certainly due to the poor preservation of the surface of the scapula. The scapula of IVPP V6028-3 has a mediolaterally thinner and slightly anteroposteriorly wider shaft than either scapula of IVPP V6027. This almost certainly is in part due to damage to the scapular shaft of IVPP V6028-3, which has been mediolaterally compressed, but may also represent slight

biological variation; however, this variation is minor, and can be regarded as intraspecific given the lack of striking morphological differences between IVPP V6027 and IVPP V6028. The scapula-coracoid suture is gently dorsally convex, with the point of maximum curvature lying around halfway along its length. The suture is clear, though the elements appear to have been firmly attached to one another.

Coracoid. IVPP V6027-3 (Fig. 6A–B) includes a left coracoid and IVPP V6028-3 (Fig. 6E–F) includes a partial right coracoid, both preserved in articulation with the corresponding scapulae. The coracoid is suboval with a single coracoid foramen (Fig. 6A–B, cof) near the dorsal margin, close to the anteroposterior midpoint of the bone. The coracoid grows mediolaterally thicker towards its contribution to the glenoid (becoming at least five times thicker than at the anteroventral corner, where the bone is thinnest), and also immediately dorsal to the coracoid foramen. The lateral surface of the coracoid immediately ventral to the glenoid is depressed. There are no notable differences between the coracoids of IVPP V6027-3 and IVPP V6028-3, other than those caused by damage

Humerus. IVPP V6027-5 (Fig.7A–F) and IVPP V6028-4 (Fig. 7G–L) are both right humeri. The angle in distal view between the deltopectoral crest and the main shaft is smaller in IVPP V6027-5 (Fig. 7E, dpc) than in *Euparkeria capensis* (SAM-PK-5867), indicating that the crest protrudes ventrally rather than ventrolaterally in the former. The crest is broken in IVPP V6028-4; it appears to be slightly more laterally directed than in IVPP V6027-5, but this is probably at least in part due to mediolateral compression of the entire proximal end of IVPP V6027-5, as evidenced by extensive cracks across the surface of the bone. The position of the crest on the

humeral shaft does not differ noticeably from that seen in *Euparkeria capensis* (SAM-PK-5867), contra Wu (1982). In lateral view (Fig. 7C) the deltopectoral crest projects ventrally as a broad triangular flange and extends to around half of the way distally along the shaft. The internal tuberosity (Fig. 7C-L, it) is visible as a rounded medial projection from near the proximal margin in ventral view in IVPP V6027-4, but appears to be less prominent in IVPP V6027-5; however, this difference is also likely to at least partly reflect mediolateral compression of the proximal end of IVPP V6027-5. The humerus lacks a distinct trochlea (=radial/lateral condyle) and capitellum (=ulnar/medial condyle); in ventral view the distal end is expanded, with a concave distal margin separating distally convex ect- and entepicondyles (Fig. 7D, ect, ent). The rugose and unfinished surface between these epicondyles would probably have borne a strip of cartilage connecting and covering the ect- and entepicondyles as in *Caiman* (see Romer 1956, Figs. 166–167), possibly with a small trochlea and capitellum formed by this cartilage. The supinator process (Fig. 7B, sup) is a low, rounded ridge extending proximally along the ventrolateral edge of the shaft from the distal end. The distal part of the supinator process may have been more prominent in life, but the surface appears to be damaged in both IVPP V6027-5 and IVPP V6028-4. Dorsal to the supinator process there is no clear ectepicondylar groove, unlike in *Erythrosuchus africanus* (Gower 2003), but this part of the surface of the humeral shaft is gently concave (Fig. 7B, ectg). It is possible that a more pronounced groove was once present distally, but is now obscured by post-mortem damage. The angle between the long axes of the distal and proximal ends of the humerus is around 20°. Whilst the deltopectoral crest and internal tuberosity may differ slightly between the specimens in terms of their direction and development respectively, there are no differences that cannot be convincingly ascribed to a combination of post-mortem damage and intraspecific variation.

534 *Ulna.* IVPP V6027-6 (Fig. 8A–F) consists of a right ulna, and IVPP V6028 includes a right ulna
535 (Fig. 8G–L) that is either IVPP V6028-7, IVPP 6028-8 or IVPP V6028-9 (it is unclear which of
536 these numbers refers to the ulna of IVPP V6028, and which ones to the radius and fibula). The
537 olecranon (Fig. 8A–L, ol) is better developed than in *Euparkeria capensis* (SAM-PK-6047) and
538 is rounded proximally. The proximal surface is convex dorsoventrally. The entire proximal end,
539 including most of the olecranon, has an unfinished surface texture and was seemingly not fully
540 ossified. The proximal end is suboval in proximal view, tapering dorsally and flattened medially.
541 The shaft is slightly twisted along its length, and has the cross-sectional shape of a dorsoventrally
542 elongated oval with a flattened medial edge. A rounded fossa midway between the dorsal and
543 ventral edges on the medial side of the shaft, near the proximal end, in IVPP V6027-6 (Fig. 8B,
544 fos) is probably an artefact of preparation rather than a genuine feature not present in the ulna of
545 IVPP V6028. The distal end is convex in lateral or medial view and straight in dorsal and ventral
546 view. In distal view the distal end is a dorsoventrally elongated oval. There is a slightly raised
547 area on the lateral surface at the proximal end of the bone (Fig. 8D–E, ra), although this swelling
548 is too poorly developed to be considered a true radial tuber. A ridge (Fig. 8D–E, ri) extends
549 distally along the shaft, beginning around 20% of the way from the proximal end and extending
550 nearly to the distal end. Ventral and parallel to this ridge runs a groove, which becomes narrower
551 distally. Bounding this groove ventrally is a second ridge, less well developed than the first,
552 which angles dorsally as it extends distally. The ridges and groove are not preserved in IVPP
553 V6028, a difference almost certainly reflecting the poor preservation of that specimen rather than
554 biological variation.

555

556 *Radius.* IVPP V6027-7 (Fig. 8C–R) is a right radius, and IVPP V6028 includes a poorly
557 preserved right radius (Fig. 8S–X; either IVPP V6028-7, IVPP V6028–8, or IVPP V6028-9, see

above). The proximal and distal ends of the shaft are formed of unfinished bone (Fig. 8M,O), and their outlines are mediolaterally expanded ovals. The proximal end is expanded further laterally than medially, and the centre of the proximal surface is depressed. The ventral surface bears a groove that extends along some 80% of the length of the bone (Fig. 8R, gr), and begins and ends roughly equidistant from each end of the radius. The dorsal surface of the radius (Fig. 8Q) is flattened along about 60% of the length of the shaft, beginning near the proximal end; this flattened area is bordered both medially and laterally by an abrupt break of slope and low ridge. The ventral part of the distal end of the radius is slightly bevelled (Fig. 8R, bev) and rugose. The distal end is convex. The radius of IVPP V6028 appears to be slightly more slender than that of IVPP V6027-7, especially distally, but this difference is largely accounted for by the smaller size of the former combined with damage to its distal end.

Femur. IVPP V6028-5 (Fig. 9) is a right femur. The shaft is sigmoidal. In distal view, the angle of offset between the long axes of the distal and proximal ends (40–50°) is greater than the corresponding angl[in] *Euparkeria capensis* (SAM-PK-6047B). The proximal end is a dorsomedially-ventrolaterally elongated oval in proximal view (Fig. 9~~A~~); the bone surface is rugose and slightly concave, indicating the presence of a large cartilaginous ~~epiphysis~~ in life. A low ridge (=medial tuber of Nesbitt 2011) extends distally along the ventral surface of the femur, beginning at the proximal margin then subsequently nearly merging indistinguishably with the bone surface, before redeveloping into a clear fourth trochanter (Fig. 9D–F, 4t). The fourth trochanter forms a laterally convex arc in ventral view. The apex of the trochanter is halfway between the proximal and distal ends of this structure and situated closer to the medial margin of the femur than to the lateral margin; the trochanter is mediolaterally widest at this point. A raised ring of bone surrounding a rugose depression that is placed lateral to the proximal end of the

trochanter (Fig. 9E, cfb) may be the area of insertion for the *m. caudofemoralis brevis*, and the trochanter itself in addition to a proximomedially adjacent rugose area (Fig. 9E, cfl) may represent the area of insertion for the *m. caudofemoralis longus* (see Romer, 1923; Hutchinson, 2001b; Schachner, Manning, & Dodson, 2011). A rounded and raised area on the lateral surface of the femur (Fig. 9B, fte), about one third of the shaft length from the proximal end, may mark the proximal part of the area of origin of the *m. femorotibialis externus* (Romer, 1923; Hutchinson, 2001b; Schachner, Manning, & Dodson, 2011). This raised area is adjacent to a slight bulge on the ventrolateral margin of the femur, referred to here as the ventral eminence (Fig. 9B, ve). The shaft has an egg-shaped cross-section, in that the ventral margin of the shaft is narrower mediolaterally than the dorsal margin and narrows further to form the adductor crest (Fig. 9D, ac) as it passes distally. The distal end of the femur is divided into lateral and medial condyles (Fig. 9E, lc, mc) that are separated by an intercondylar groove distally (Fig. 9 ~~C~~, ig) and dorsally, and by a shallowly depressed popliteal space ventrally (Fig.9~~E~~, ps). The lateral condyle bears a tapered, ventrally projecting *crista tibiofibularis* (Fig. 9~~E~~, ct). The bone surface of the distal end (Fig. 9 ~~C~~) is rugose, indicating a large cartilaginous epiphysis in life.

Tibia. IVPP V6028-6 (Fig. 10A–F) is a right tibia. The proximal end of the tibia is around twice as expanded dorsoventrally and mediolaterally as the distal end. The proximal end has relatively straight dorsomedial, dorsolateral and ventrolateral edges and a convexly curved ventromedial edge in proximal view (Fig. 10A). The dorsal margin of the proximal end is expanded to form a cnemial crest (Fig. 10A, cn), whereas the ventrolateral corner of the proximal end is very slightly expanded to form an indistinct posterior condyle (Fig. 10A, pc). The proximal surface of the tibia is convex overall, but is interrupted by a dorsoventrally elongated concavity that is closer to the lateral margin of the proximal surface than the medial margin. The shaft of the tibia

displays a dorsally convex curvature in lateral view (Fig. 10D). The cross-sectional shape of the shaft is a mediolaterally compressed ellipse. As preserved, the distal end of the tibia has the outline of an oval elongated along a ventrolateral-to-dorsomedial axis (Fig. 10C), and is slightly concave to flat. No definite attachment site for the *m. puboischiotibialis* can be identified (unlike the condition in *Erythrosuchus africanus*, Gower 2003). There is a step (Fig. 10F, step) on the medial surface of the tibia, beginning around one quarter of the way down the shaft. This step separates the more prominent ventral part of the medial surface of the tibia from the more subdued dorsal part.

Fibula. IVPP V6028 includes a right fibula (Fig. 10G–L; either IVPP V6028-7, IVPP V6028–8, or IVPP V6028-9, see above). The fibula is long and slender (ratio of shaft diameter to shaft length is lower than in, e.g., *Batrachotomus kupferzellensis*: Gower and Schoch 2009, fig. 6K–N), relatively straight, and flattened mediolaterally. The proximal end of the fibula is missing, but the proximalmost preserved part of the bone bears an eminence on the lateral surface (Fig. 10J, m.if) that was interpreted by Wu (1982) as the insertion site for the *m. iliofibularis* (corresponding to the anterior trochanter of e.g. Borsuk-Białynicka & Sennikov 2009). This interpretation is plausible, but the attachment would then be more proximally positioned than in most stem and early archosaurs (e.g., Nesbitt 2011: fig. 41). A possible exception is *Osmolskina* (Borsuk-Białynicka & Sennikov 2009), but no fibula has been assigned to this taxon with more than tentative certainty. However, a proximally placed *m. iliofibularis* insertion is characteristic of derived pseudosuchians (e.g. *Crocodylus niloticus*: Borsuk-Białynicka & Sennikov 2009). The shaft tapers mediolaterally and dorsoventrally for more than half of its preserved length before reexpanding distally. The long axes of the distal part of the shaft and the proximalmost preserved part are offset by around 75°. The shaft is oval in cross-section, but the dorsal surface is pinched

to form an elongated ridge (Fig. 10G, ri). The distal end of the shaft is strongly expanded ventrolaterally to dorsomedially, and the ventrolateral margin of the distal end is much wider in distal view than the dorsomedial margin. A small groove (Fig. 10K, ?gr) runs proximodistally along the ventral surface of the fibula near the distal end, though this may be an artefact of poor preservation. In lateral view, the distal margin of the fibula is embayed between dorsal and ventral rounded convexities. The lateral surface of the distal end is depressed at its dorsoventral midpoint.

Median osteoderms. IVPP V6027-1 (Fig.4A–E) and IVPP V6027-2 (Fig. 4F–J) include median osteoderms in articulation with cervicodorsal and dorsal vertebrae, respectively, and IVPP V6027-9 (Fig. 5E–F) is an isolated median osteoderm. The osteoderms form two parallel rows that contact one another along the midline (Fig. 4B,G). The osteoderms are similar to those of *Euparkeria capensis* (UMZC T.692; Fig. 5G–H) in each possessing a medially offset longitudinal keel (Fig. 5E,K), in being leaf shaped, and in that each osteoderm dorsally overlaps the immediately more posterior one in the same row. Each osteoderm is around twice as long anteroposteriorly as it is wide mediolaterally. Each osteoderm overlaps the neural spines of two vertebrae (Fig. 4B,G), covering the anterior third of the spine of the more posterior vertebra and the posterior two thirds of the spine of the more anterior vertebra. Adjacent left and right osteoderms are, as in *Euparkeria capensis* (SAM-PK-13666) level with each other anteroposteriorly rather than staggered

Phylogenetic relationships of *Halazhaisuchus qiaoensis* and '*Turfanosuchus*' *shageduensis*

Our initial phylogenetic analysis (Fig. 11) including *Halazhaisuchus qiaoensis* and '*Turfanosuchus*' *shageduensis* as separate taxa yielded 810 most parsimonious trees (MPTs) of 1257 steps with a consistency index (CI) of 0.384 and a retention index (RI) of 0.793. *Halazhaisuchus qiaoensis* and '*Turfanosuchus*' *shageduensis* were found to be sister taxa, forming a clade that was in turn placed as sister to *Euparkeria capensis*. This result is consistent with our recognition of '*Turfanosuchus*' *shageduensis* as a junior subjective synonym of *Halazhaisuchus qiaoensis*. It also supports a monophyletic Euparkeriidae, consisting of *Euparkeria capensis* and *Halazhaisuchus qiaoensis*, that forms the sister clade to Archosauria+Phytosauria. However, Euparkeriidae is supported only by one local apomorphy: character 407, presacral osteoderms that are longer than wide. The sister grouping of *Halazhaisuchus qiaoensis* and '*Turfanosuchus*' *shageduensis* is also supported by a single local apomorphy: 219, teardrop-shaped tuber on posterior edge of scapula present (following the wording of Nesbitt 2011 – the tuber is in fact circular, but is almost certainly homologous with the teardrop shaped tubera of other taxa). Bootstrap support for the node Archosauria+Phytosauria is >~~50~~%, with a Bremer support of three, but bootstrap support for Euparkeriidae and for *Halazhaisuchus qiaoensis*+'*Turfanosuchus*' *shageduensis* is <50% and Bremer support for both nodes is one. Seven extra steps were required to find a monophyletic clade composed of '*Turfanosuchus*' *shageduensis*, *Halazhaisuchus qiaoensis* and *Turfanosuchus dabanensis* (whether or not '*Turfanosuchus' shageduensis* and *Halazhaisuchus qiaoensis* were constrained to be sister taxa). Nineteen extra steps were required to recover a monophyletic Euparkeriidae composed of a combined *Halazhaisuchus qiaoensis*, '*Turfanosuchus*' *shageduensis*, *Turfanosuchus dabanensis* and *Euparkeria capensis* (whether or not '*Turfanosuchus' shageduensis* and *Halazhaisuchus qiaoensis* were constrained to be sister taxa).

The topology (excepting of course the sister group relationship of the two taxa in question) and character optimization were identical when *Halazhaisuchus qiaoensis* and '*Turfanosuchus*' *shageduensis* were combined as a single taxon, and support values differed only slightly (Bremer support of four for Archosauria+Phytosauria). This analysis recovered 270 MPTs of 1276 steps with a CI of 0.379 and an RI of 0.787. *Turfanosuchus dabanensis* was placed as the sister taxon of *Gracilisuchus*+*Yonghesuchus* within Pseudosuchia, as found by Butler et al. (2014). Seven extra steps were required to place *Turfanosuchus dabanensis* as the sister taxon to the combined *Halazhaisuchus qiaoensis*. Nineteen extra steps were required to recover a monophyletic Euparkeriidae composed of a combined *Halazhaisuchus qiaoensis* OTU, *Turfanosuchus dabanensis* and *Euparkeria capensis*.

Discussion

We consider *Wangisuchus tzeyii* to be a *nomen dubium* due to the undiagnostic nature of the holotype material. Whilst some of the material currently assigned to the taxon may indeed pertain to a euparkeriid or euparkeriid-grade species, the specimens are too fragmentary and poorly preserved for a reasonable assessment of their systematic position to be made. The problem is compounded by the lack of convincing evidence that any of the different specimens pertain to the same individual or taxon, especially given that other archosauromorphs (e.g. *Shansisuchus shansisuchus*) were collected from the same localities and strata.

Although the fragmentary nature of the material complicates taxonomic reassessment, the type specimens of *Halazhaisuchus qiaoensis* and '*Turfanosuchus' shageduensis* are not sufficiently morphologically distinct to justify maintaining both taxa, and we consider them

synonymous. This synonymy is supported by our numerical cladistic analysis which places the two putative species as sister taxa, and by the similar size and stratigraphic position of the taxa. However, it must be stressed that there are limited numbers of overlapping elements between the taxa showing sufficiently good preservation to draw conclusions, and that the holotypes are from different sites - future discoveries of better preserved material from the lower Ermaying could thus potentially refute this synonymization. It must also be noted that only a single synapomorphy, the presence of a tuber for muscle attachment on the posterior edge of the scapula, currently supports the sister group relationship between the synonymized taxa when they are treated as separate OTUs. This tuber is clearly present in the holotype of *Halazhaisuchus qiaoensis* and appears to be present in the holotype of '*Turfanosuchus' shageduensis*, but is not well preserved in the latter. Despite the limited extent of the evidence for synonymy, we believe that the lack of countervailing evidence means that it remains the more parsimonious hypothesis. Even were synonymy to be subsequently refuted, given their generally similar morphology, size and stratigraphic position it can be safely concluded that both taxa are stem archosaurs of a similar "ancestral-archosaur" grade.

Our phylogenetic analysis constitutes only the third test of the existence of a monophyletic, non-monospecific Euparkeriidae, the first being an analysis by Ezcurra, Lecuona, & Martinelli (2010) that included the putative euparkeriids *Osmolskina czatkowicensis* and *Euparkeria capensis* but did not find them to be sister taxa, and the second being an analysis by Sookias et al. (2014) that included the putative euparkeriids *Dorosuchus neoetus* and *Euparkeria capensis* but did not find them to be sister taxa. As a result, our analysis is the first to recover a monophyletic, non-monospecific euparkeriid clade. Our ongoing work is focused on developing a more extensive dataset to simultaneously test the positions of *Euparkeria capensis*, *Dorosuchus*

723 *neoetus*, *Halazhaisuchus qiaoensis*, and *Osmolskina czatkowicensis*, but this is beyond the scope
724 of the current pa

725 Whilst *Halazhaisuchus qiaoensis* and *Euparkeria capensis* form a clade in our analysis,
726 this result must be considered provisional as only two of the putative euparkeriid taxa were
727 included in the analysis and support for the clade was low, with osteoderm shape constituting the
728 only synapomorphy of the clade. The osteoderms of *Halazhaisuchus qiaoensis* and *Euparkeria*
729 *capensis* are indeed very similar, being leaf-shaped and possessing medially offset longitudinal
730 keels. Moreover, the osteoderms are arranged almost identically in the two taxa, forming in each
731 case two paramedian rows slightly out of step with the spine tables below them. However,
732 *Euparkeria capensis* differs from *Halazhaisuchus qiaoensis* in lacking the pronounced scapular
733 tuber for muscle attachment that is an apparent autapomorphy of the latter taxon, and in more
734 subtle aspects of shape in several elements (e.g. *Euparkeria capensis* has a less well developed
735 olecranon process of the ulna, and a slightly less strongly expanded distal end of the scapula). It
736 should also be noted that our scoring for osteoderm shape differs from that of Nesbitt (2011:
737 character 407), who scored the osteoderms of *Euparkeria capensis* as "square-shaped, about
738 equal dimensions" rather than "longer than wide". We disagree with this scoring as the maximum
739 width to maximum length ratio of the paramedian osteoderms of *Euparkeria capensis* is 0.43
740 (UMZC T.692j). This is similar to the value for *Batrachotomus kupferzellensis* (0.46, SMNS
741 90018), which Nesbitt (2011) scored as having elongated osteoderms, but strikingly different
742 from that for *Hesperosuchus agilis* (0.72, AMNH FR 6758, measured from fig. 50 in Nesbitt
743 2011) which Nesbitt (2011) scored as having square-shaped osteoderms. The width to length ratio
744 is 0.47 in *Halazhaisuchus qiaoensis* (IVPP V6027-8), again more similar to the condition in
745 *Batrachotomus kupferzellensis* than that in *Hesperosuchus agilis*.

746 The incomplete nature of the material of *Halazhaisuchus qiaoensis* makes ecological
747 inferences difficult. The animal can be estimated to have been around 1.5 m in length, based on
748 length estimates for *Euparkeria capensis* (Ewer 1965; Botha-Brink and Smith 2011; Remes
749 2007) scaled according to the length ratio between the single femur referred to *Halazhaisuchus*
750 *qiaoensis* (127 mm) and the longest femur of *Euparkeria capensis* (78 mm, SAM-PK-10671).
751 *Halazhaisuchus qiaoensis* was also probably carnivorous, based on the apparently cylindrical
752 shape of the preserved teeth, though no details of dental morphology can be discerned. Similar
753 locomotor ability as has been posited for *Euparkeria capensis*, namely quadrupedal locomotion
754 and possibly facultative bipedality at speed (Ewer 1965; Santi 1993), can be tentatively ascribed
755 to *Halazhaisuchus qiaoensis*: the humerus/femur ratio (1.51 for IVPP V6028), femoral length as
756 percentage of femur+tibia length (55% for IVPP V6028), and humerus+ulna length as a
757 percentage of femur+tibia length (69% for IVPP V6028) are similar to the corresponding values
758 for *Euparkeria capensis* (1.40, approximately 63%, and 67%, respectively; Gauthier et al. 2011,
759 Ewer 1965). Femoral morphology is also similar, though the tibia is less symmetrical
760 mediolaterally than that of *Euparkeria capensis*. Lack of preservation of the pelvic girdle
761 precludes further conclusions regarding locomotor ability.

762 Our reassessment of the putative Chinese Euparkeriidae helps to shed light on character
763 evolution leading up to the origin of archosaurs. Together with *Euparkeria capensis*, the
764 morphology of *Halazhaisuchus qiaoensis* probably approaches that of the common ancestor of
765 Phytosauria+Archosauria. Whilst the locomotor apparatus of *Euparkeria capensis* and
766 *Halazhaisuchus qiaoensis* is not specialized for fully upright or bipedal locomotion, unlike that of
767 early dinosauriforms and pseudosuchians (see Gauthier et al. 2011), it departs from that of more
768 sprawling taxa, with reduction and ventral displacement of the fourth trochanter. Based on
769 *Halazhaisuchus qiaoensis* and *Euparkeria capensis*, the ancestor of Archosauria and phytosaurs

can also be hypothesised to have been relatively small and gracile, terrestrial, and probably carnivorous. The vertebrae of *Halazhaisuchus qiaoensis* show some structures that correspond to the extensive laminae and fossae of Archosauria and phytosaurs, features that have often, but controversially, been considered to indicate the presence of pneumatic diverticula (see Butler, Barrett, & Gower 2012), but in *Halazhaisuchus qiaoensis* these structures are not particularly well developed. *Halazhaisuchus qiaoensis*, along with *Euparkeria capensis*, is intermediate in development of vertebral laminae and fossae between the archosaurs and phytosaurs on the one hand and more basal taxa such as *Proterosuchus fergusi* on the other. However, laminae and fossae are better developed in *Erythrosuchus africanus* than in Euparkeriidae (Gower 2003; Butler, Barrett, & Gower 2012) despite the more crownward placement of the latter, implying that the elaboration of laminae and fossae in archosauriform evolution (whether related to pneumaticity or not) did not follow a simple trend.

Acknowledgements

The authors thank K. Tang (University College London) for assistance with Chinese language names.

Funding

R.B.S. and R.J.B. are supported by an Emmy Noether Programme Award from the Deutschen Forschungsgemeinschaft (BU 2587/3-1 to R.J.B.) and by a Marie Curie Career Integration Grant

(PCIG14-GA-2013-630123 ARCHOSAUR RISE to R.J.B.). C.S. and L.J. are supported by the Institute of Vertebrate Paleontology and Paleoanthropology of the Chinese Academy of Sciences, Beijing.

References

~~Alcober~~ O. 2000. Redescription of the skull of *Saurosuchus galilei* (Archosauria: Rauisuchidae). *Journal of Vertebrate Paleontology* 20:302-316.

Bennett SC. 1996. The phylogenetic position of the Pterosauria within the Archosauromorpha. *Zoological Journal of the Linnean Society* 118:261-308.

Benton MJ. 1999. *Scleromochlus taylori* and the origin of the dinosaurs and pterosaurs. *Philosophical Transactions of the Royal Society of London B* 354:1423-1446.

Benton MJ, Donoghue PCJ. 2007. Paleontological evidence to date the tree of life. *Molecular Biology and Evolution* 24:26-53.

Borsuk-Białynicka M, Sennikov AG. 2009. Archosauriform postcranial remains from the Early Triassic karst deposits of southern Poland. *Palaeontologia Polonica* 65:283-328.

813 Botha-Brink J, Smith RMH. 2011. Osteohistology of the Triassic archosauromorphs *Prolacerta*,
814 *Proterosuchus*, *Euparkeria*, and *Erythrosuchus* from the Karoo Basin of South Africa. *Journal of*
815 *Vertebrate Paleontology* 31:1238-1254.
816
817 Butler RJ, Brusatte S L, Reich M, Nesbitt SJ, Schoch RR, Hornung JJ. 2011. The sail-backed
818 reptile *Ctenosauriscus* from the latest Early Triassic of Germany and the timing and
819 biogeography of the early archosaur radiation. *PLoS ONE* 6: e25693.
820
821 Butler RJ, Barrett PM, Gower DJ. 2012. Reassessment of the evidence for postcranial skeletal
822 pneumaticity in Triassic archosaurs, and the early evolution of the avian respiratory system. *PLoS*
823 *ONE* 7: e34094.
824
825 Butler RJ, Sullivan C, Ezcurra MD, Liu J, Lecuona A, Sookias RB. 2014. New clade of enigmatic
826 early archosaurs yields insights into early pseudosuchian phylogeny and the biogeography of the
827 archosaur radiation. *BMC Evolutionary Biology* 14:128.
828
829 Brusatte SL, Benton MJ, Desojo JB, Langer MC. 2010. The higher-level phylogeny of the
830 Archosauria (Tetrapoda: Diapsida). *Journal of Systematic Palaeontology* 8:3-47.
831
832 Carrier DR, Farmer CG. 2000. The evolution of pelvic aspiration in archosaurs. *Paleobiology*
833 26:271-293.
834

835 Cohen KM, Finney S, Gibbard PL. 2013. International Chronostratigraphic Chart 2013/01.
836 International Commission on Stratigraphy.

837

838 Ferojo J B, Ezcurra MD, Schultz CL. 2011. An unusual new archosauriform from the Middle-
839 Late Triassic of southern Brazil and the monophyly of Doswellidae. *Zoological Journal of the*
840 *Linnean Society* 161:839-871.

841

842 Ewer RF. 1965.The anatomy of the thecodont reptile *Euparkeria capensis* Broom. *Philosophical*
843 *Transactions of the Royal Society of London B* 248:379-435.

844

845 Ezcurra MD, Lecuona A, Martinelli A. 2010. A new basal archosauriform diapsid from the Lower
846 Triassic of Argentina. *Journal of Vertebrate Paleontology* 30:1433–1450.

847

848 Foth C, Rauhut OWM. 2013. Macroevolutionary and morphofunctional patterns in theropod
849 skulls: a morphometric approach. *Acta Palaeontologica Polonica* 58:1-16.

850

851 Fröbisch J. 2009. Composition and similarity of global anomodont-bearing tetrapod faunas.
852 *Earth-Science Reviews* 95:119-157.

853

854 Gauthier JA. 1986. Saurischian monophyly and the origin of birds. *Memoirs of the California*
855 *Academy of Sciences* 8:1-55.

856

857 Gauthier JA, Kluge AG, Rowe T. 1988. Amniote phylogeny and the importance of fossils.

Cladistics 4:105–209.

Gauthier JA, Nesbitt SJ, Schachner ER, Bever GS, Joyce WG. 2011. The bipedal stem crocodilian *Poposaurus gracilis*: inferring function in fossils and innovation in archosaur locomotion. *Bulletin of the Peabody Museum of Natural History* 52:107-126.

Goloboff PA, Farris JS, Nixon K. 2003. TNT: tree analysis using new technologies. Program and documentation available from the authors. Available at http://www.zmuc.dk/public/phylogeny (accessed 19 July 2014)

Goloboff PA, Farris JS, Nixon K. 2008. TNT: a free program for phylogenetic analysis. *Cladistics* 24:774-786.

Gower DJ. 2000. Rauisuchian archosaurs (Reptilia, Diapsida): an overview. *Neues Jahrbuch für Geologie und Paläontologie Abhandlungen* 218:447-488.

Gower DJ. 2003.Osteology of the early archosaurian reptile *Erythrosuchus africanus* Broom. *Annals of the South African Museum* 111:1-88.

Gower DJ, Schoch R. 2009. Postcranial anatomy of the rauisuchian archosaur *Batrachotomus kupferzellensis*. *Journal of Vertebrate Paleontology* 29:103-122.

Gower DJ, Sennikov AG. 2000. Early archosaurs from Russia. In: Benton MJ, Shishkin MA, Unwin DM, Kurochkin EN, eds. *The age of dinosaurs in Russia and Mongolia*. New York: Cambridge University Press, 140–159.

Gower DJ, Wilkinson M. 1996. Is there any consensus on basal archosaur phylogeny? *Proceedings of Royal Society of London B* 263:1399-1406.

Hancox PJ. 1998. A stratigraphic, sedimentological and palaeonvironmental synthesis of the Beaufort-Molteno contact in the Karoo Basin. Ph.D. Thesis, University of the Witwatersrand.

Hancox PJ. 2000. The continental Triassic of South Africa. *Zentralblatt für Geologie und Paläontologie* Teil I, 1998:1285-1324.

Hancox PJ, Angielczyk KD, Rubidge BS. 2013. *Angonisaurus* and *Shansiodon*, dicynodonts (Therapsida, Anomodontia) from Subzone C of the *Cynognathus* Assemblage Zone (Middle Triassic) of South Africa. *Journal of Vertebrate Paleontology* 33:655-676.

Hocknull SA, Piper PJ, van den Bergh GD, Due RA, Morwood MJ, et al. 2009. Dragon's paradise lost: palaeobiogeography, evolution and extinction of the largest-ever terrestrial lizards (Varanidae). *PLoS ONE* 4: e7241

Huene F von.1920. Osteologie von *Aëtosaurus ferratus* O. Fraas. *Acta Zoologica* 1:465-491.

Huene F von. 1946. Die großen Stämme der Tetrapoden in den geologischen Zeiten. *Biologisches Zentralblatt* 65:268-275.

Huene F von. 1956. Paläontologie und Phylogenie der niederen Tetrapoden. Jena: VEB Gustav

907 Fischer Verlag.

908

909 Hutchinson JR. 2001a. The evolution of pelvic osteology and soft tissues on the line to extant

910 birds (Neornithes). *Zoological Journal of the Linnean Society* 131:123-168.

911

912 Hutchinson JR. 2001b. The evolution of femoral osteology and soft tissues on the line to extant

913 birds (Neornithes). *Zoological Journal of the Linnean Society* 131:123-168.

914

915 Krebs B. 1976. Pseudosuchia. In: Kuhn O, ed. *Handbuch der Paläoherpetologie*. Stuttgart/New

916 York: Gustav Fischer Verlag. 40–98.

917

918 Kuhn O. 1976. Handbuch der Paläoherpetologie. Stuttgart/New York: Gustav Fischer Verlag.

919

920 Liu J, Zhao Y, Liu X, Wang Y, Liu X. 2012. Rapid exhumation of basement rocks along the

921 northern margin of the North China craton in the Early Jurassic: evidence from the Xiabancheng

922 Basin, Yanshan Tectonic Belt. *Basin Research* 24:544-558.

923

924 Liu J, Li L, Li X-W. 2013. SHRIMP U-Pb zircon dating of the Triassic Ermaying and Tongchuan

925 formations in Shanxi, China and its stratigraphic implications. *Vertebrata Palasiatica* 51:162-

926 168.

927

928 Lucas SG. 1998. Global Triassic tetrapod biostratigraphy and biochronology. *Palaeontology,*

929 *Palaeoclimatology, Palaeoecology* 143:347-384.

930

931 Lucas SG. 2001. *Chinese fossil vertebrates*. New York: Columbia University Press.

932

933 Lucas SG. 2010. The Triassic timescale based on nonmarine tetrapod biostratigraphy and

934 biochronology. In: Lucas SG, ed. *The Triassic timescale*. London: Geological Society, Special

935 Publications 334, 447–500.

936

937 Lucas SG, Hunt AP. 1993. *Fukangolepis* Yang, 1978 from the Triassic of China is not an

938 aetosaur. *Journal of Vertebrate Paleontology* 13:145-147.

939

940 Maidment SCR, Barrett P M. 2011. The locomotor musculature of basal ornithischian dinosaurs.

941 *Journal of Vertebrate Paleontology* 31:1265-1291.

942

943 Marugán-Lobón J, Buscalioni ÁD. 2003. Disparity and geometry of the skull in Archosauria

944 (Reptilia: Diapsida). *Zoological Journal of the Linnean Society* 80:67-88.

945

946 Nesbitt SJ. 2003. *Arizonasaurus* and its implications for archosaur divergence. *Proceedings of*

947 *the Royal Society of London B. 2*70:S234-S237.

948

949 Nesbitt SJ. 2011. The early evolution of archosaurs: relationships and the origin of major clades.

950 *Bulletin of the American Museum of Natural History* 352:1-292.

951

952 Nesbitt SJ, Liu J, Li C. 2011. A sail-backed suchian from the Heshanggou Formation (Early

953 Triassic: Olenekian) of China. *Earth and Environmental Science Transactions of the Royal*
954 *Society of Edinburgh* 110:271-284.
955
956 Nesbitt SJ, Brusatte SL, Desojo J B, Liparini A, De França MA, Weinbaum J C, Gower D J.
957 2013. Rauisuchia. In: Nesbitt SJ, Desojo BJ, Irmis RB, eds. *Anatomy, phylogeny and*
958 *palaeobiology of early archosaurs and their kin.* London: Geological Society, Special
959 Publications 379, 241–274.
960
961 Norman DB, Weishampel DB. 1991. Feeding mechanisms in some small herbivorous dinosaurs:
962 processes and patterns. In: Rayner JMV, Wootton RJ, eds. *Biomechanics in evolution*. Cambridge:
963 Cambridge University Press, 161–181.
964
965 Parrish JM. 1986. Locomotor adaptations in the hindlimb and pelvis of Thecodontia. *Hunteria*
966 1:1-35.
967
968 Parrish JM. 1992. Phylogeny of the Erythrosuchidae (Reptilia: Archosauriformes). *Journal of*
969 *Vertebrate Paleontology* 12:93-102.
970
971 Parrish MJ. 1993. Phylogeny of the Crocodylotarsi, with reference to archosaurian and
972 crurotarsan monophyly. *Journal of Vertebrate Paleontology* 13:287-308.
973
974 Parrish J M. 1997. Archosauria. In: Currie PJ, Padian K, eds. *Encyclopedia of dinosaurs*. London:
975 Academic Press, 20–24.
976
977 Perry SF. 1992. Gas exchange strategies in reptiles and the origin of the avian lung. In: Wood SC,

978 Weber RE, Hargens AR, Millard RW, eds. *Physiological adaptations in vertebrates: respiration,*
979 *circulation, and metabolism*. New York: Marcel Dekker, 149–167.
980
981 Rauhut OWM. 2003. The interrelationships and evolution of basal theropod dinosaurs. *Special*
982 *Papers in Palaeontology* 69:1-213.
983
984 Remes K. 2007. Evolution of the pectoral girdle and forelimb in Sauropodomorpha (Dinosauria,
985 Saurischia): osteology, myology and function. Ph.D. thesis, Ludwig Maximilian University of
986 Munich.
987
988 Romer AS. 1956. *Osteology of the Reptiles*. Chicago: University of Chicago Press.
989
990 Romer AS. 1972.The Chañares (Argentina) Triassic reptile fauna. XIII. An early ornithosuchid
991 pseudosuchian, *Gracilisuchus stipanicicorum*, gen. et sp. nov. Breviora 389:1-24.
992
993 Renaut AJ, Hancox PJ. 2001.Redescription of *Kannemeyeria argentinensis* (Therapsida,
994 Dicynodontia). *Palaeontologia africana* 37:81-91.
995
996 Rewcastle SC. 1980. Form and function in lacertilian knee and mesotarsaljoints: a contribution to
997 the analysis of sprawling locomotion. *Journal of Zoology* 191:147-170.
998
999 de Ricqlès A, Padian K, Knoll F, Horner J R. 2008. On the origin of high growth rates in
1000 archosaurs and their ancient relatives: complementary histological studies on Triassic
1001 archosauriforms and the problem of a “phylogenetic signal” in bone histology. *Annales de*
1002 *Paléontologie* 94:57-76.

1003

1004 Romer AS. 1923. Crocodilian pelvic muscles and their avian and reptilian homologues. *Bulletin*

1005 *of the American Museum of Natural History* 48:533-552.

1006

1007 Romer AS. 1942. The development of tetrapod limb musculature-the thigh of *Lacerta. Journal of*

1008 *Morphology* 71:251-298.

1009

1010 Romer AS. 1972. The Chañares (Argentina) Triassic reptile fauna. XVI. Thecodont classification.

1011 *Breviora* 395:1-24.

1012

1013 Renaut AJ, Hancox PJ. 2001. Redescription of *Kannemeyeria argentinensis* (Therapsida,

1014 Dicynodontia). *Palaeontologia africana* 37:81-91.

1015

1016 Rubidge BS. 2005. Re-uniting lost continents – fossil reptiles from the ancient Karoo and their

1017 wanderlust. *South African Journal of Geology* 108:135-172.

1018

1019 Santi G. 1993. Functional bipedalism in some Permo-Triassic extinct reptiles: a possible scale of

1020 the degree of efficiency. *Studi Trentini di Scienze Naturali Acta Biologica* 68:267-280.

1021

1022 Schachner ER, Manning PL, Dodson P. 2011. Pelvic and hindlimb myology of the basal

1023 archosaur *Poposaurus gracilis* (Archosauria: Poposauroidea). *Journal of Morphology* 272:1464-

1024 1491.

1025

1026 Sulej T. 2005. A new rauisuchian reptile (Diapsida: Archosauria) from the Late Triassic of

1027 Poland. *Journal of Vertebrate Paleontology* 25:78-86.

1028

1029 Sennikov AG. 1989a. Novyy euparkeriid (Thecodontia) iz srednego triasa Yuzhnogo Priural'ya.

1030 *Paleontologicheskiy Zhurnal* 1989:71-78.

1031

1032 Sennikov AG. 1989b. A new euparkeriid (Thecodontia) from the Middle Triassic of the Southern

1033 Urals. *Paleontological Journal* 22:66-73.

1034

1035 Seymour RS, Bennett-Stamper CL, Johnston SD, Carrier DR, Grigg GC. 2004. Evidence for

1036 endothermic ancestors of crocodiles at the stem of archosaur evolution. *Physiological and*

1037 *Biochemical Zoology* 77:1051-1067.

1038

1039 Shubin NH, Sues HD. 1991. Biogeography of early Mesozoic continental tetrapods: patterns and

1040 implications. *Paleobiology* 214-230.

1041

1042 Sookias RB, Sennikov AG, Gower DJ, Butler RJ (2014). The monophyly of Euparkeriidae

1043 (Reptilia: Archosauriformes) and the origins of crown Archosauria: a revision of *Dorosuchus*

1044 *neoetus* from the Middle Triassic of Russia. *Palaeontology* (published online).

1045

1046 Spielmann JA, Lucas SG, Heckert AB, Rienhart LF, Richards III HR. 2009. Redescription of

1047 *Spinosuchus caseanus* (Archosauromorpha: Trilophosauridae) from the Upper Triassic of North

1048 America. *Palaeodiversity* 2:283-31

1049

1050 Sues H-D, Fraser NC. 2010. Triassic Life on Land: the Great Transition. New York: Columbia

1051 University Press.

1052

1053 Sullivan C. 2010. The role of the calcaneal ‘heel’ as a propulsive lever in basal archosaurs and
1054 extant monitor lizards. *Journal of Vertebrate Paleontology* 30:1422-1432.
1055
1056 Welles SP, Long RA. 1974.The tarsus of theropod dinosaurs. *Annals of the South African*
1057 *Museum* 64:191-218.
1058
1059 Wilson JA. 1999. A nomenclature for vertebral laminae in sauropods and other saurischian
1060 dinosaurs. *Journal of Vertebrate Paleontology* 19:639-653.
1061
1062 Wilson JA, D’Emic MD, Ikejiri T, Moacdieh EM, Whitlock JA. 2011. A nomenclature for
1063 vertebral fossae in sauropods and other saurischian dinosaurs. *PLoS ONE* 6:e17114.
1064
1065 Wu X. 1981. The discovery of a new thecodont form North−East Shensi. *Vertebrata PalAsiatica*
1066 19:122-132. (in Chinese with English summary)
1067
1068 Wu X. 1982. The pseudosuchian reptiles from Shan−Gan−Ning basin. *Vertebrata PalAsiatica*
1069 20:289-301. (in Chinese with English summary)
1070
1071 Wu X-C, Russell AP. 2001. Redescription of *Turfanosuchus* ~~dabanensis~~ (Archosauriformes) and
1072 new information on its phylogenetic relationships. *Journal of Vertebrate Paleontology* 21:40-50.
1073
1074 Wu X-C, Sues H-D. 1996. Reassessment of *Platyognathus hsui* Young, 1944 (Archosauria:
1075 Crocodyliformes) from the Lower Lufeng Formation (Lower Jurassic) of Yunnan, China. *Journal*
1076 *of Vertebrate Paleontology* 16:42-48.
1077

1078 Wu X, Sun A. 2008. Infraclass Archosauromorpha. In: Li J, Wu X, Zhang F, eds. 2008. *The*
1079 *Chinese fossil reptiles and their kin*. Beijing: Science Press, 167–214.
1080
1081 Wu X-C, Liu J, Li J. 2001.The anatomy of the first archosauriform (Diapsida) from the terrestrial
1082 Upper Triassic of China. *Vertebrata PalAsiatica* 39:251-265.
1083
1084 Yin H-f. 2003. Triassic Biostratigraphy of China. In: Zhang W, Chen P-j, Palmer AR, eds.
1085 *Biostratigraphy of China*. Beijing: Science Press, 379–422.
1086
1087 Young CC [Yang Z]. 1944. On a supposed new pseudosuchian from Upper Triassic saurischian-
1088 bearing Red Beds of Lufeng, Yunnan, China. *American Museum Novitates* 1264:1-4.
1089
1090 Young CC [Yang Z]. 1964. The pseudosuchians in China. *Palaeontologia Sinica* 151:S1-205.
1091
1092 Young CC [Yang Z]. 1973. On a new pseudosuchian from Turfan, Sinkiang. *Memoirs of the*
1093 *Institute of Vertebrate Palaeontology and Paleoanthropology Academia Sinica* 10:15-38.
1094
1095 Young CC [Yang Z]. 1978. A Late Triassic vertebrate fauna from Fu-kang, Sinkiang. *Memoirs of*
1096 *the Institute of Vertebrate Paleontology and Paleoanthropology Academia Sinica* 13:60-67.
1097
1098 Zhen S, Zhen B, Master NJ, Lucas SG. 1985. The Mesozoic reptiles of China. In: Lucas SG,
1099 Master NJ, eds. *Studies of Chinese fossil vertebrates*. Uppsala: Bulletin of the Geological
1100 Institutions of the University of Uppsala, 11, 133–150.
1101
1102 **Figure captions**

1103

1104 Figure 1. **Localities of the putative Chinese euparkeriids**. Map showing the localities where
1105 the holotype specimens of the three Chinese putative euparkeriid taxa reassessed in this paper
1106 were collected. Pale grey=People's Republic of China; darker grey=other countries; cross-
1107 hatched light and darker grey=disputed regions; dark grey=ocean; thick grey lines=national
1108 borders; thin grey lines=province borders; stars=localities.

1109

1110 Figure 2. **Holotype and paratypes of "*Wangisuchus tzeyii*" *nomen dubium***. Holotype IVPP
1111 V2701, left maxilla, in medial (A) and lateral (B) views. Paratypes, right maxillae, in lateral
1112 views: IVPP V2702 (C); IVPP V2703 (D); IVPP V2704 (E). al, alveolus, aofo, antorbital fossa,
1113 idp, interdental plate, mas, ascending process of the maxilla, t, tooth.

1114

1115 Figure 3. **Mandible of *Halazhaisuchus***. Right mandible of *Halazhaisuchus qiaoensis*, IVPP
1116 V6028-1 (holotype of '*Turfanosuchus*' *shageduensis*) in lateral (A), medial (B) and dorsal (C)
1117 views. a, angular, c, coronoid, d, dentary, pa, prearticular, sa, surangular, sp, splenial, step, step
1118 between more dorsal and more ventral sections of prearticular, t, teeth.

1119

1120 Figure 4. **Cervical and dorsal vertebrae of *Halazhaisuchus qiaoensis***. Posterior three cervical
1121 and anterior three dorsal vertebrae IVPP V6027-1 in right lateral (A), dorsal (B; osteoderms
1122 visible), ventral (C), anterior (D) and posterior (E) views; series of dorsal vertebrae IVPP V6027-
1123 2 in right lateral (F), dorsal (G; osteoderms visible), ventral (H), anterior (I) and posterior (J)
1124 views; cervical vertebrae of IVPP V6028-2 (holotype of '*Turfanosuchus*' *shageduensis*) in right
1125 lateral (K; broken segments disarticulated), ventral (L), dorsal (M), anterior (N) and posterior (O)
1126 views. acpl, anterior centroparapophyseal lamina, di, diapophysis, ep, epipophysis, ic,
1127 intercentrum, ns, neural spine, ost, osteoderm, pa, parapophysis, ppdl, paradiapophyseal lamina,

1128 prdl, prezygodiapophyseal lamina, sdf, spinodiapophyseal fossa, tp, transverse process.

1129

1130 Figure 5. **Ribs and osteoderms of *Halazhaisuchus* compared with other taxa.** Right cervical
1131 rib of *Halazhaisuchus qiaoensis* IVPP V6027-9 in dorsal (A) and ventral (B) views; left cervical
1132 rib (image mirrored for comparison) of *Batrachotomus kupferzellensis* SMNS 91046 in dorsal
1133 (C) and ventral (D) views; right paramedian osteoderm of *Halazhaisuchus qiaoensis* IVPP
1134 V6027-8 in dorsal (E) and ventral (F) views; right paramedian osteoderm of *Euparkeria capensis*
1135 UMZC T692j in dorsal (G) and ventral (H) views. cap, capitulum, fl, flange, k, keel, tub,
1136 tuberculum.

1137

1138 Figure 6. **Scapulae and coracoids of *Halazhaisuchus qiaoensis***. Left scapula and coracoid IVPP
1139 V6027-3 in lateral (A) and medial (B) views, right scapula and partial coracoid IVPP V6027-4 in
1140 lateral (C) and medial (D) views, and left scapula and coracoid IVPP V6028-3 (holotype of
1141 '*Turfanosuchus*' *shageduensis*) in lateral (E) and medial (F) views. acr, acromion process, cof,
1142 coracoid foramen, gl, glenoid, mar, muscle attachment ridge, tu, tuber.

1143

1144 Figure 7. **Right humeri of *Halazhaisuchus qiaoensis***. IVPP V6027-5 in proximal (A), dorsal
1145 (B), lateral (C), ventral (D), distal (E) and medial (F) views, and IVPP V6028-4 (holotype of
1146 '*Turfanosuchus*' *shageduensis*) in proximal (G), dorsal (H), lateral (I), ventral (j), distal (K) and
1147 medial (L) views. Arrows indicate dorsal direction. ectg, ectepicondylar groove, ect,
1148 ectepicondyle, ent, entepicondyle, dpc, deltopectoral crest, it, internal tuberosity.

1149

1150 Figure 8. **Right forelimb epipodials of *Halazhaisuchus qiaoensis***. Ulna IVPP V6027-6 in
1151 proximal (A), medial (B), distal (C), lateral (D), dorsal (E), and ventral (F) views; ulna of IVPP
1152 V6028 (holotype of '*Turfanosuchus*' *shageduensis*) in proximal (G), medial (H), distal (I), lateral

(J), dorsal (K), and ventral (L) views; radius IVPP V6027-7 in proximal (M), medial (N), distal (O), lateral (P), dorsal (Q), and ventral (R) views; radius of IVPP V6028 (holotype of '*Turfanosuchus*' *shageduensis*) in proximal (S), medial (T), distal (U), lateral (V), dorsal (W), and ventral (X) views. Arrows indicate dorsal direction. bev, bevelled surface, fos, fossa, gr, groove, ol, olecranon, ra, raised area, ri, ridge.

Figure 9. **Femur of *Halazhaisuchus***. Right femur of *Halazhaisuchus qiaoensis* IVPP V6028-5 (holotype of '*Turfanosuchus*' *shageduensis*) in dorsal (A), proximal (B), lateral (C), ventral (D), medial (E) and distal (F) views. Arrows indicate dorsal direction. ac, adductor crest, cfb, *m. caudofemoralis brevis* attachment, cfl, *m. caudofemoralis longus* attachment, ct, crista tibiofibularis, fte, m. femorotibialis externus attachment, h, head, ig, intercondylar groove, lc, lateral condyle, mc, medial condyle, ps, popliteal space, ve, ventral eminence, 4t, fourth trochanter.

Figure 10. **Right hind limb epipodials of *Halazhaisuchus qiaoensis***. Tibia IVPP V6028-6 (holotype of '*Turfanosuchus*' *shageduensis*) in proximal (A), dorsal (B), distal (C), lateral (D), ventral (E) and medial (F) views; fibula of IVPP V6028 (holotype of '*Turfanosuchus*' *shageduensis*) in dorsal (G), distal (H), proximal (I), lateral (J), ventral (K) and medial (L) views. Arrows indicate dorsal direction. cn, cnemial crest, lc, lateral condyle, m.if, *m. iliofibularis* attachment, pc, posterior condyle, ri, ridge, step, step between more medial and more lateral surfaces, ?gr, possible groove.

Figure 11. **Phylogenetic position of *Halazhaisuchus***. Strict consensus of 810 most parsimonious trees of length 1257 steps, showing the phylogenetic positions of *Halazhaisuchus qiaoensis* and

1177 '*Turfanosuchus*' *shageduensis*. Consistency index=0.384; retention index=0.793. Numbers below
1178 nodes are bootstrap values (before the slash) and decay indices (after the slash) for the nodes in
1179 question.

1180

1181 **SI Captions**

1182

1183 Table S1. **Supplementary table of measurements.** Measurements of specimens referred to
1184 *Halazhaisuchus qiaoensis* and of holotype and paratypes of "*Wangisuchus tzeyii*".

1185

1186 Table S2. **Supplementary table of Chinese names.** Names of localities, towns, administrative
1187 divisions and formations used in this article, showing their equivalents in simplified Chinese,
1188 Pinyin, and previously published romanizations and translations.

1189

1190 Matrix S1. **Character matrix.** Matrix based on that of Butler et al. (2014) with scores for
1191 *Halazhaisuchus qiaoensis* and '*Turfanosuchus*' *shageduensis*, as well as for a single
1192 *Halazhaisuchus* OTU (incorporating '*Turfanosuchus*' *shageduensis* as a junior subjective
1193 synonym).

Figure 1

Localities of the putative Chinese euparkeriids.

Map showing the localities where the holotype specimens of the three Chinese putative euparkeriid taxa reassessed in this paper were collected. Pale grey=People's Republic of China; darker grey=other countries; cross-hatched light and darker grey=disputed regions; dark grey=ocean; thick grey lines=national borders; thin grey lines=province borders; stars=localities.

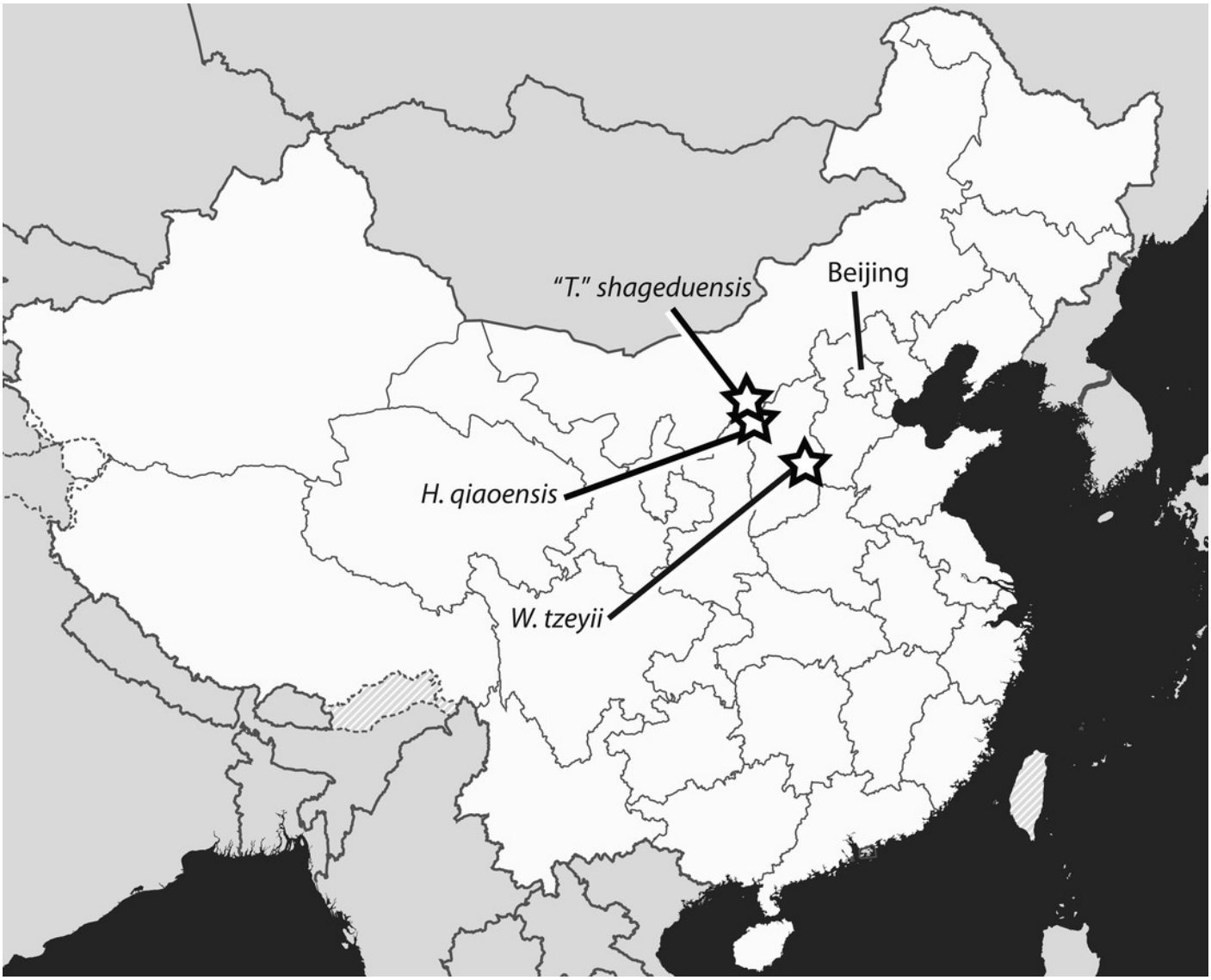

Figure 2

Holotype and paratypes of “*Wangisuchus tzeyii*” *nomen dubium.*

Holotype IVPP V2701, left maxilla, in medial (A) and lateral (B) views. Paratypes, right maxillae, in lateral views: IVPP V2702 (C); IVPP V2703 (D); IVPP V2704 (E). al, alveolus, aofo, antorbital fossa, idp, interdental plate, mas, ascending process of the maxilla, t, tooth.

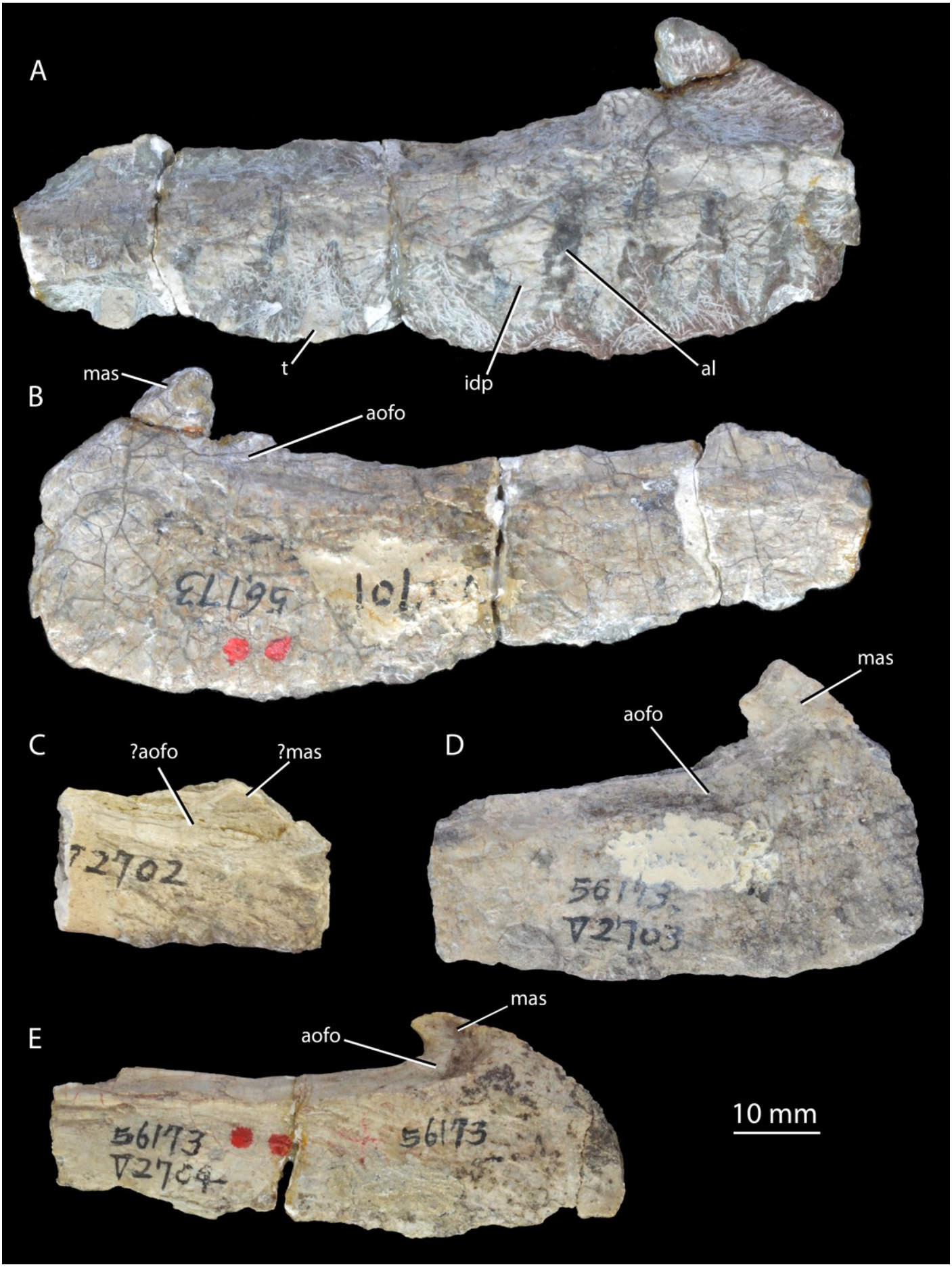

Figure 3

Mandible of *Halazhaisuchus qiaoensis*.

Right mandible of *Halazhaisuchus qiaoensis*, IVPP V6028-1 (holotype of 'Turfanosuchus shageduensis) in lateral (A), medial (B) and dorsal (C) views. a, angular, c, coronoid, d, dentary, pa, prearticular, sa, surangular, sp, splenial, step, step between more dorsal and more ventral sections of prearticular, t, teeth.

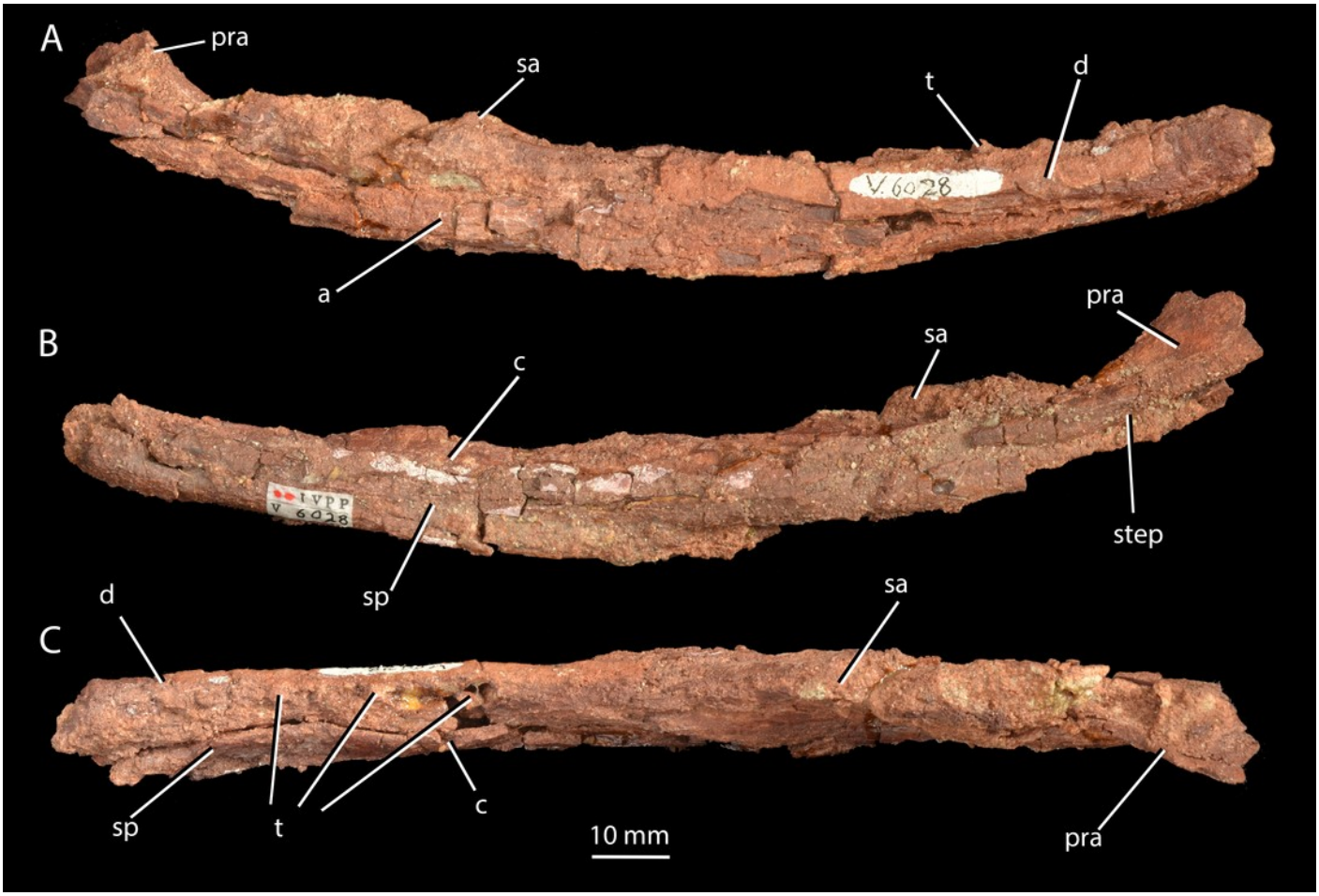

Figure 4

Cervical and dorsal vertebrae of *Halazhaisuchus qiaoensis*.

Posterior three cervical and anterior three dorsal vertebrae IVPP V6027-1 in right lateral (A), dorsal (B; osteoderms visible), ventral (C), anterior (D) and posterior (E) views; series of dorsal vertebrae IVPP V6027-2 in right lateral (F), dorsal (G; osteoderms visible), ventral (H), anterior (I) and posterior (J) views; cervical vertebrae of IVPP V6028-2 (holotype of '*Turfanosuchus*' *shageduensis*) in right lateral (K; broken segments disarticulated), ventral (L), dorsal (M), anterior (N) and posterior (O) views. acpl, anterior centroparapophyseal lamina, di, diapophysis, ep, epipophysis, ic, intercentrum, ns, neural spine, ost, osteoderm, pa, parapophysis, ppdl, paradiapophyseal lamina, prdl, prezygodiapophyseal lamina, sdf, spinodiapophyseal fossa, tp, transverse process.

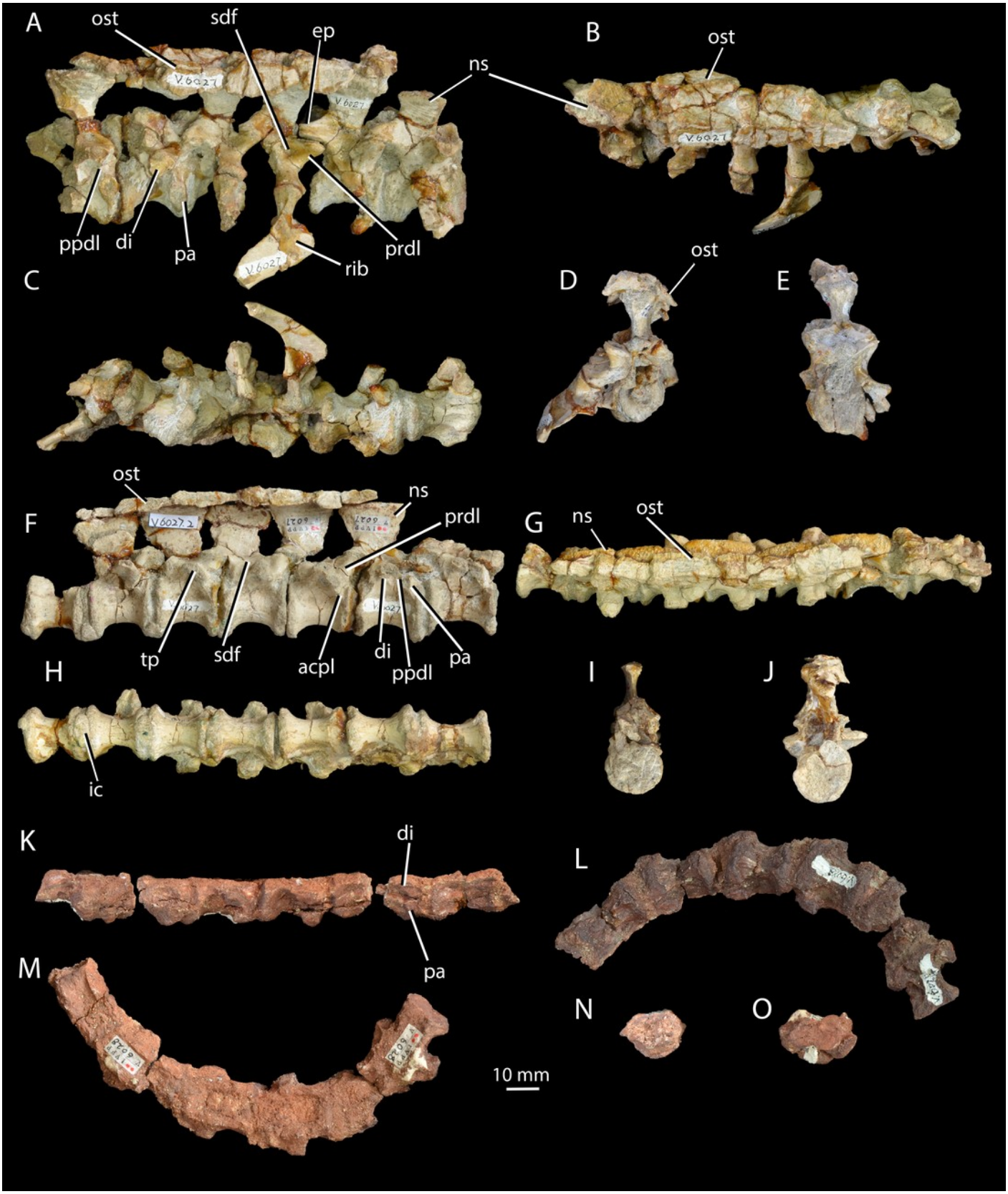

Figure 5

Rib and osteoderm of *Halazhaisuchus qiaoensis* compared with other taxa.

Right cervical rib of *Halazhaisuchus qiaoensis* IVPP V6027-9 in dorsal (A) and ventral (B) views; left cervical rib (image mirrored for comparison) of Batrachotomus kupferzellensis SMNS 91046 in dorsal (C) and ventral (D) views; right paramedian osteoderm of *Halazhaisuchus qiaoensis* IVPP V6027-8 in dorsal (E) and ventral (F) views; right paramedian osteoderm of *Euparkeria capensis* UMZC T692j in dorsal (G) and ventral (H) views. cap, capitulum, fl, flange, k, keel, tub, tuberculum.

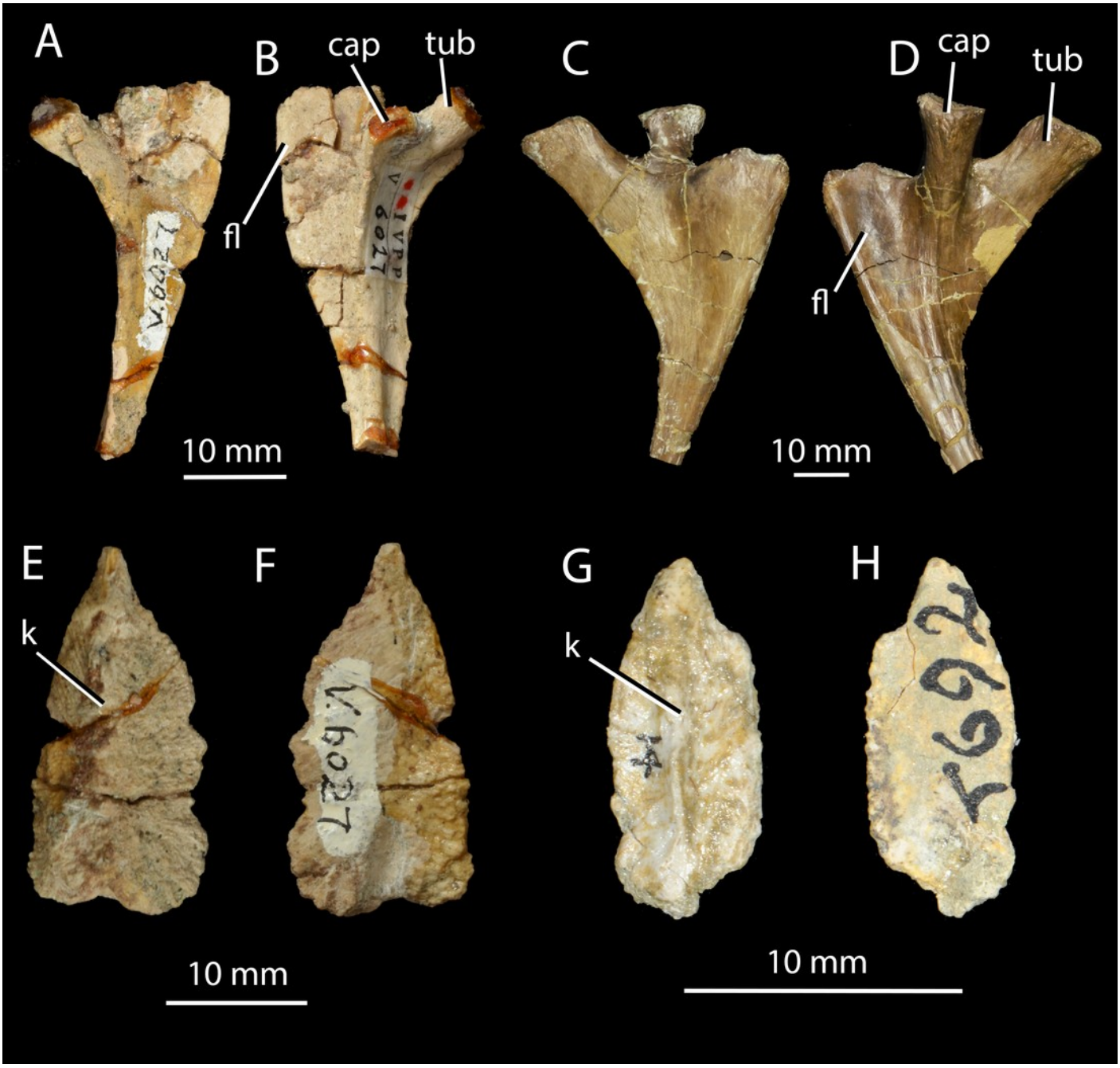

Figure 6

Scapulae and coracoids of *Halazhaisuchus qiaoensis*.

Left scapula and coracoid IVPP V6027-3 in lateral (A) and medial (B) views, right scapula and partial coracoid IVPP V6027-4 in lateral (C) and medial (D) views, and left scapula and coracoid IVPP V6028-3 (holotype of '*Turfanosuchus*' *shageduensis*) in lateral (E) and medial (F) views. acr, acromion process, cof, coracoid foramen, gl, glenoid, mar, muscle attachment ridge, tu, tuber.

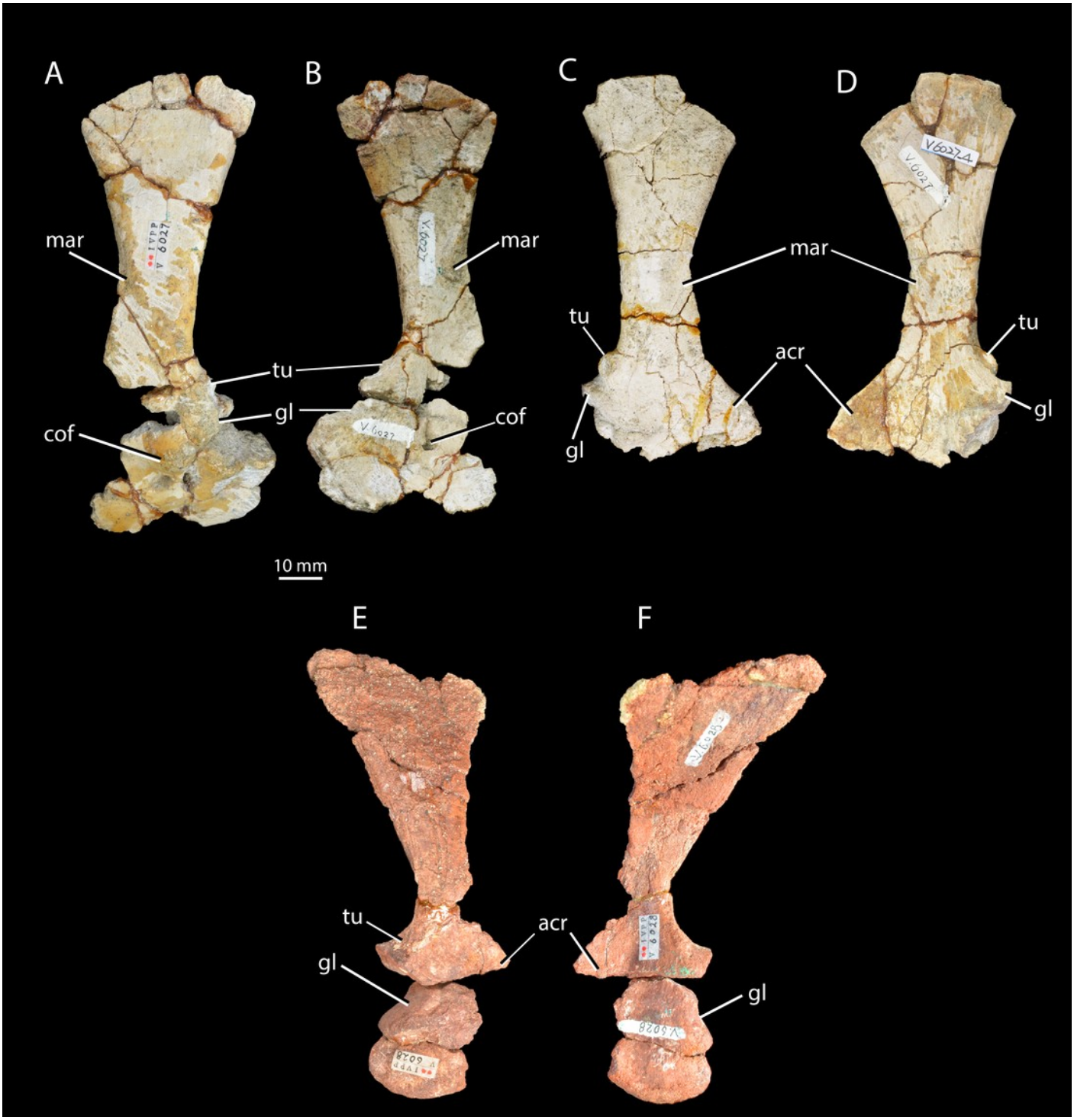

Figure 7

Right humeri of *Halazhaisuchus qiaoensis.*

IVPP V6027-5 in proximal (A), dorsal (B), lateral (C), ventral (D), distal (E) and medial (F) views, and IVPP V6028-4 (holotype of '*Turfanosuchus*' *shageduensis*) in proximal (G), dorsal (H), lateral (I), ventral (j), distal (K) and medial (L) views. Arrows indicate dorsal direction. ectg, ectepicondylar groove, ect, ectepicondyle, ent, entepicondyle, dpc, deltopectoral crest, it, internal tuberosity

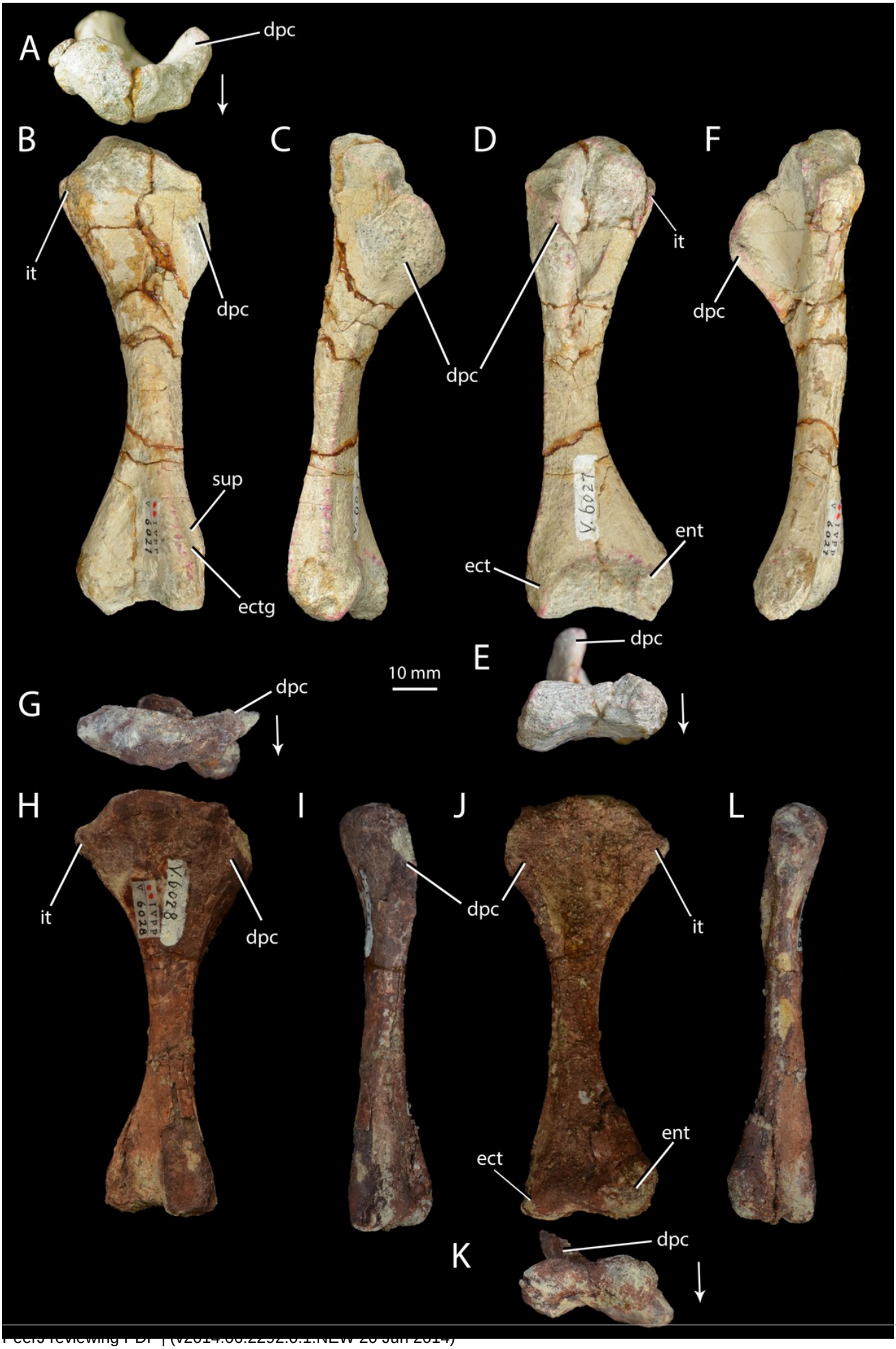

Figure 8

Right forelimb epipodials of *Halazhaisuchus qiaoensis*.

Ulna IVPP V6027-6 in proximal (A), medial (B), distal (C), lateral (D), dorsal (E), and ventral (F) views; ulna of IVPP V6028 (holotype of '*Turfanosuchus*' *shageduensis*) in proximal (G), medial (H), distal (I), lateral (J), dorsal (K), and ventral (L) views; radius IVPP V6027-7 in proximal (M), medial (N), distal (O), lateral (P), dorsal (Q), and ventral (R) views; radius of IVPP V6028 (holotype of '*Turfanosuchus*' *shageduensis*) in proximal (S), medial (T), distal (U), lateral (V), dorsal (W), and ventral (X) views. Arrows indicate dorsal direction. bev, bevelled surface, fos, fossa, gr, groove, ol, olecranon, ra, raised area, ri, ridge.

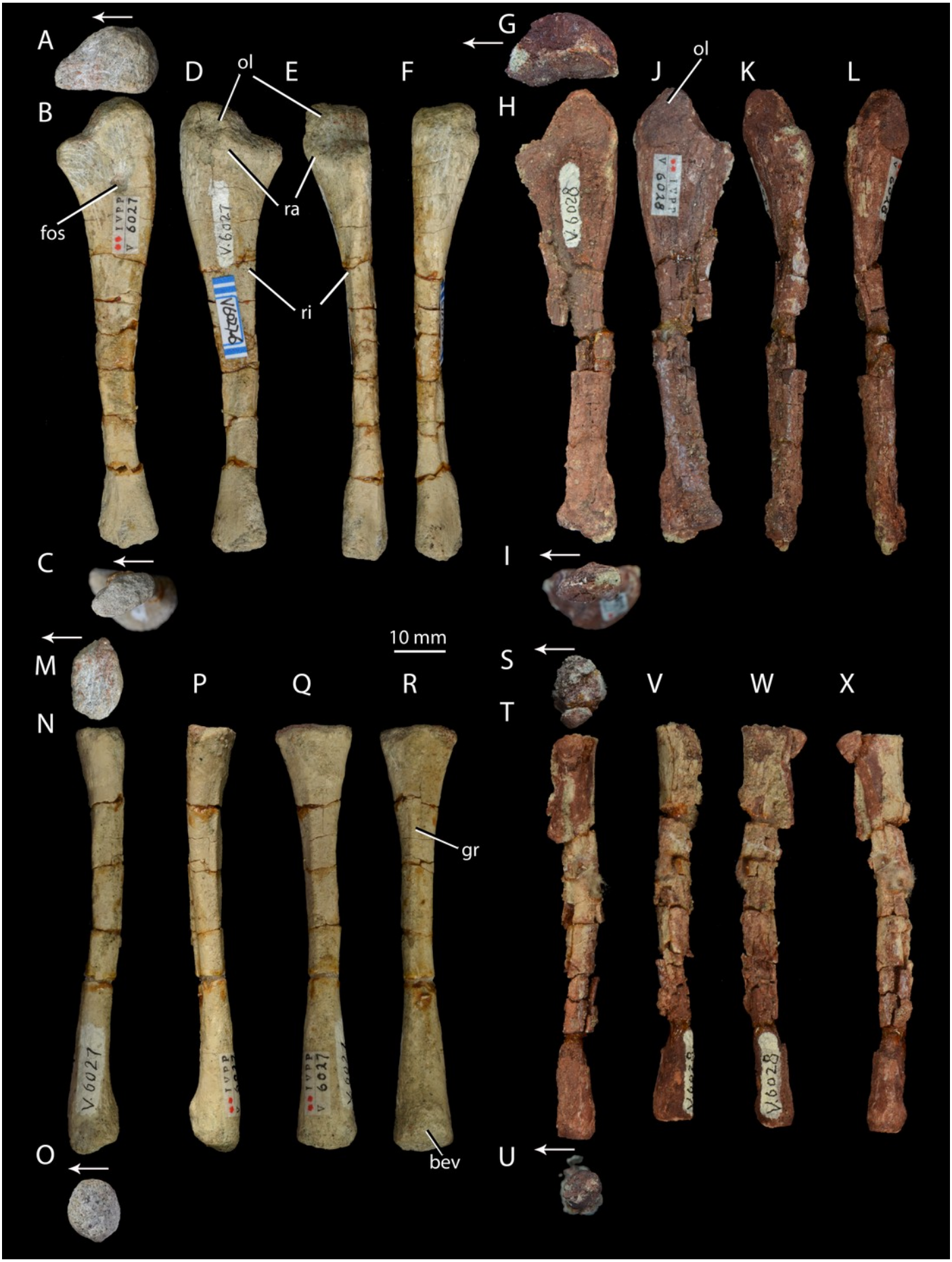

Figure 9

Femur of *Halazhaisuchus qiaoensis*.

Right femur of *Halazhaisuchus qiaoensis* IVPP V6028-5 (holotype of '*Turfanosuchus*' *shageduensis*) in dorsal (A), proximal (B), lateral (C), ventral (D), medial (E) and distal (F) views. Arrows indicate dorsal direction. ac, adductor crest, cfb, m. caudofemoralis brevis attachment, cfl, m. caudofemoralis longus attachment, ct, crista tibiofibularis, fte, m. femorotibialis externus attachment, h, head, ig, intercondylar groove, lc, lateral condyle, mc, medial condyle, ps, popliteal space, ve, ventral eminence, 4t, fourth trochanter.

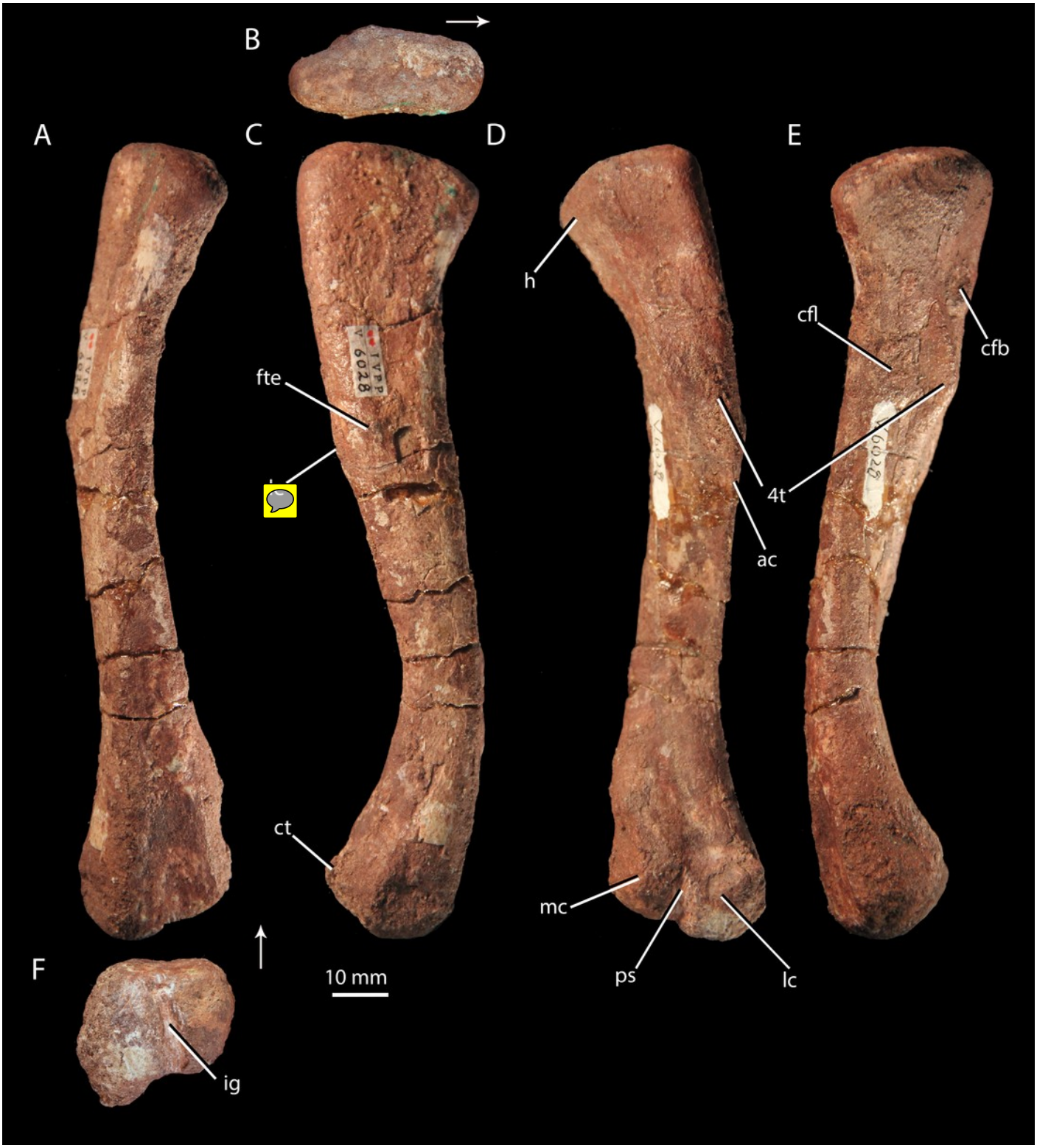

Figure 10

Right hind limb epipodials of *Halazhaisuchus qiaoensis*.

Tibia IVPP V6028-6 (holotype of '*Turfanosuchus*' *shageduensis*) in proximal (A), dorsal (B), distal (C), lateral (D), ventral (E) and medial (F) views; fibula of IVPP V6028 (holotype of '*Turfanosuchus*' *shageduensis*) in dorsal (G), distal (H), proximal (I), lateral (J), ventral (K) and medial (L) views. Arrows indicate dorsal direction. cn, cnemial crest, lc, lateral condyle, m.if, m. iliofibularis attachment, pc, posterior condyle, ri, ridge, step, step between more medial and more lateral surfaces, ?gr, possible groove.

Figure 11

Phylogenetic position of *Halazhaisuchus qiaoensis*.

Strict consensus of 810 most parsimonious trees of length 1257 steps, showing the phylogenetic positions of *Halazhaisuchus qiaoensis* and '*Turfanosuchus*' *shageduensis*. Consistency index=0.384; retention index=0.793. Numbers below nodes are bootstrap values (before the slash) and decay indices (after the slash) for the nodes in question.